ABSTRACT

LIU, TIANCONG. Scaling of Earthquake Ground Motions for Fragility Analysis of Piping Systems. (Under the direction of Abhinav Gupta).

Performance-based seismic assessment requires scaling of recorded earthquake ground motions to conduct nonlinear response time history analysis. A key objective of the scaling procedure is to preserve the distribution (both the median and the dispersion) in the earthquake shaking for the selected characterization of the hazard to enable appropriate consideration of distribution in responses and demands for the structural and the nonstructural systems. Over the past decades, suitability of various scaling methods has been evaluated by application to structural systems particularly buildings. The economic loss due to failure of nonstructural components could be more than 50% of total loss. This paper presents the results from a study that compares and contrasts the applicability of a couple of different widely used scaling methods as well as some of the recently proposed methods to a nonstructural (piping) system installed inside a building. These methods are: (i) Single period scaling method, (ii) “Range” based scaling method, (iii) Geometric mean based scaling method, (iv) Distribution based scaling method. Several different aspects are considered for comparing these methods particularly with respect to the dynamic characteristics of nonstructural systems. Seismic fragilities of piping system are calculated and compared for each individual scaling method by using nonlinear time history response analyses. The failure limit-state considered in these analyses is taken directly from the existing experimental data on nonlinear behavior of threaded T-joints. Finally, a new ground motion scaling method which addressed the deficiencies of the existing scaling methods is proposed.

Scaling of Earthquake Ground Motions for Fragility Analysis of Piping Systems

by
Tiancong Liu

A thesis submitted to the Graduate Faculty of
North Carolina State University
in partial fulfillment of the
requirements for the degree of
Master of Science

Civil Engineering

Raleigh, North Carolina

2015

APPROVED BY:

_____	_____
Dr. James Nau	Dr. Shamim Rahman

_____
Dr. Abhinav Gupta
Chair of Advisory Committee

DEDICATION

To My Family

BIOGRAPHY

Tiancong Liu was born on Oct 1, 1989 and grew up in Hangzhou, China. Being a witness of 2008 Sichuan Earthquake that saw more than 80,000 people dead due to inadequately designed buildings, he chose the major of Civil Engineering after National Higher Education Entrance Examination. He dreams of contributing to reducing and possibly eliminating casualties during future earthquake disasters. He received a Bachelor of Science (with honors) in Civil Engineering at Guangxi University in June, 2012. He decided to further his education in United States and started his Master's program at North Carolina State University in Aug, 2012. He joined the research group of Dr. Abhinav Gupta and concentrated on seismic analysis of nonstructural piping systems since May, 2013.

Tiancong plans to realize his professional objective in industry after completion of graduate study. Upon graduation, he is scheduled to start working with The Harman Group (THG) in King of Prussia, PA as a design engineer.

ACKNOWLEDGMENTS

I would like to express my sincere gratitude to my advisor, Dr. Abhinav Gupta, for giving me this opportunity to pursue a master's degree in Civil Engineering at North Carolina State University while maintain my research interest in earthquake engineering. His constant guidance during my research work and thesis writing through my graduate study cannot be expressed by few words. I would like to express my appreciation and respect for him helping me throughout the research. I would also like to thank Dr, James Nau and Dr. Shamim Rahman for their time by agreeing to serve on my committee.

I would also like to thank other members in Dr. Gupta's research group, Payel Chatterjee, Shinyoung Kwag and Harleen Sandhu, for their help especially with questions related to earthquake engineering. Their assistance helped me make faster progress in my graduate research.

My parents, although unable to understand my research at NCSU, constantly motivate me to fulfill my responsibility as a graduate student, as a researcher and soon as an entry level engineer. I would never forget their unselfish love, their sacrifices their financial support as well as their faith in myself ever since I started my study abroad. I could never imagine making it through without their confidence in myself. Very special thanks should be given to my best friend Yuxiang Li who is a PhD candidate in University of Cincinnati. He has been my best friend ever since senior high school and always helps me out when I'm in need. There are clearly some other friends working in industry or studying in other institutes that I would like to acknowledge. It would not have been possible to complete my graduate study without their support.

TABLE OF CONTENTS

LIST OF TABLES……...vii

LIST OF FIGURES……viii

PART I: INTRODUCTION……...1

1. Introduction 2

2. Objective 4

3. Proposed Research 5

4. Organization 6

References 8

PART II: SCALING OF EARTHQUAKE GROUND MOTIONS FOR FRAGILITY ANALYSIS OF PIPING SYSTEMS……...10

1. Introduction 11

2. Significance of Nonstructural Systems and Their Characteristics 14

3. Piping System Configuration, Limit-State, and Dynamic Characteristics 17

4. Selection of Earthquake Ground Motions 21

5. Methods for Scaling Ground Motions 24

5.1. Single Period Scaling Method (Sa(T_i) Scaling Method) 24

5.2. Multiple Period Scaling Method (“Range” Scaling Method) 25

5.3. Geometric Mean Scaling Method 26

5.4. Distribution Scaling Method 26

6. Assessment of Scaling Methods 29

6.1. Single Period Scaling..... 29

6.2. Multiple Period Scaling Method ("Range" Scaling Method)..... 31

6.3. Geometric Mean Scaling Method..... 31

6.4. Distribution Scaling Method (D-Scaling Method) 32

6.5. Non-Uniqueness of D-Scaling Method 33

7. Piping Fragility for Different Scaling Methods 34

8. Proposed Scaling Method 38

9. Proposed Method for Fragility Assessment..... 39

10. Summary and Conclusions..... 42

References 45

PART III: SUMMARY AND CONCLUSIONS……...105

1. Summary and Conclusions 106

1.1. Summary..... 106

1.2. Conclusions 108

2. Recommendations for Future Research..... 110

References 111

LIST OF TABLES

PART II: SCALING OF EARTHQUAKE GROUND MOTIONS FOR FRAGILITY ANALYSIS OF PIPING SYSTEMS

Table 1: First 20 period (sec) /frequencies (HZ) of the piping system 48

Table 2: Degaggregation bin details (% hazard) 48

Table 3: 21 selected ground motion records 49

Table 4: Periods considered for “Range” based scaling method 49

LIST OF FIGURES

Figure 1: Piping System Configuration with Threaded Tee-joint at Single Location……..50

Figure 2: Characterization of Limit State (Ju, 2012) 51

Figure 3: Rotations of 2-inch Black Iron Tee-joint for "First Leak" failure in Cyclic Tests (Ju, 2012)..... 52

Figure 4: Hospital Piping System Layout (Ju, 2012)..... 53

Figure 5: Global Fundamental Mode Shape, Local Fundamental Mode Shape and Local Second Mode Shape Of the Piping System..... 54

Figure 6: UHS with 2% of exceedance in 50 years at site of interest using USGS online hazard application (longitude 117.856 W, latitude 34.102, site class: C)..... 55

Figure 7: Probabilistic seismic hazard deaggregation at site of interest generated using 2002 version USGS interactive deaggregation tools (USGS, 2008b)..... 56

Figure 8: Median response spectrum (RS) of 21 unscaled ground motions versus 2% UHS and corresponding median predicted UHS..... 57

Figure 9: Logarithmic standard deviation (β) of 21 unscaled ground motions at the site of interest versus target β 58

Figure 10a: Selected 21 ground motions scaled to match target 2% UHS at T_{p3}=0.315s... 59

Figure 10b: Logarithmic standard deviation (β) of Sa(T_{p3}=0.315s) scaled 21 ground motions at the site of interest versus target β 60

Figure 11a: Selected 21 ground motions scaled to match target 2% UHS over specified period range 61

Figure 11b: Logarithmic standard deviation (β) of "Range" scaled 21 ground motions at the site of interest versus target β 62

Figure 12a: Selected 21 ground motions scaled to match target 2% UHS by geomean scaling method 63

Figure 12b: Logarithmic standard deviation (β) of geometric mean scaled 21 ground motions at the site of interest versus target β 64

Figure 13: "Median" predicted UHS versus 2% UHS 65

Figure 14: Example PDF and CDF for target spectral ordinates determination using D-Scaling method 66

Figure 15a: Selected 21 ground motions scaled to match target 2% UHS at T_{p9}=0.136s ... 67

Figure 15b: Logarithmic standard deviation (β) of Sa(T_{p9}=0.136s) scaled 21 ground motions at the site of interest versus target β 68

Figure 16a: Selected 21 ground motions scaled to match target 2% UHS at T_{b1}=2.07s (partial scale) 69

Figure 16b: Selected 21 ground motions scaled to match target 2% UHS at T_{b1}=2.07s (full scale) 70

Figure 16c: Logarithmic standard deviation (β) of Sa(T_{b1}=2.07s) scaled 21 ground motions at the site of interest versus target β 71

Figure 17a: Selected 21 ground motions scaled to match median predicted UHS at T_{p3}=0.315s 72

Figure 17b: Logarithmic standard deviation (β) of D-scaled 21 ground motions at the site of interest versus target β (targets at T_{p3}=0.315s) 73

Figure 18a: Selected 21 ground motions scaled to match median predicted UHS at T_{p3}=0.315s 74

Figure 18b: Logarithmic standard deviation (β) of Magnitude ordered D-scaled 21 ground motions at the site of interest versus target β (targets at T_{p3}=0.315s) 75

Figure 19a: Selected 21 ground motions scaled to match median predicted UHS at T_{p3}=0.315s 76

Figure 19b: Logarithmic standard deviation (β) of PGA ordered D-scaled 21 ground motions at the site of interest versus target β (targets at T_{p3}=0.315s) 77

Figure 20a: Selected 21 ground motions scaled to match median predicted UHS at T_{p3}=0.315s 78

Figure 20b: Logarithmic standard deviation (β) of SA ordered D-scaled 21 ground motions at the site of interest versus target β (targets at T_{p3}=0.315s) 79

Figure 21: Nonlinear seismic fragility from Sa(T_{p3}) scaled ground motions 80

Figure 22: Nonlinear seismic fragility from Sa(T_{p9}) scaled ground motions 81

Figure 23: Nonlinear seismic fragility from Sa(T_{b1}) scaled ground motions 82

Figure 24: Nonlinear seismic fragility from "Range" scaled ground motions 83

Figure 25: Nonlinear seismic fragility from geomean scaled ground motions 84

Figure 26: Nonlinear seismic fragility from D-scaled ground motions 85

Figure 27: Nonlinear seismic fragility from Magnitude ordered D-scaled ground motions86

Figure 28: Nonlinear seismic fragility from PGA ordered D-scaled ground motions 87

Figure 29: Nonlinear seismic fragility from SA ordered D-scaled ground motions 88

Figure 30: Seismic fragility from different scaling methods listed in this study (Part I).... 89

Figure 31: Seismic fragility from different scaling methods listed in this study (Part II) .. 90

Figure 32: Seismic fragility from different scaling methods listed in this study (Part III) . 91

Figure 33a: Selected 21 ground motions scaled to match median predicted UHS 92

Figure 33b: Logarithmic standard deviation (β) of proposed scaled 21 ground motions at the site of interest versus target β 93

Figure 34: Seismic fragility of piping Tee-joint from unscaled ground motions: nonlinear FE analysis versus probabilistic analysis 94

Figure 35: Seismic fragility of piping Tee-joint from single period (T_{p3}) scaled ground motions: nonlinear FE analysis versus probabilistic analysis 95

Figure 36: Seismic fragility of piping Tee-joint from single period (T_{p9}) scaled ground motions: nonlinear FE analysis versus probabilistic analysis 96

Figure 37: Seismic fragility of piping Tee-joint from single period (T_{b1}) scaled ground motions: nonlinear FE analysis versus probabilistic analysis 97

Figure 38: Seismic fragility of piping Tee-joint from "Range" based scaled ground motions: nonlinear FE analysis versus probabilistic analysis 98

Figure 39: Seismic fragility of piping Tee-joint from geometric mean based scaled ground motions: nonlinear FE analysis versus probabilistic analysis (same as unscaled case) 99

Figure 40: Seismic fragility of piping Tee-joint from D-scaled ground motions: nonlinear FE analysis versus probabilistic analysis 100

Figure 41: Seismic fragility of piping Tee-joint from Magnitude ordered D-scaled ground motions: nonlinear FE analysis versus probabilistic analysis 101

Figure 42: Seismic fragility of piping Tee-joint from PGA ordered D-scaled ground motions: nonlinear FE analysis versus probabilistic analysis 102

Figure 43: Seismic fragility of piping Tee-joint from SA ordered D-scaled ground motions: nonlinear FE analysis versus probabilistic analysis 103

Figure 44: Seismic fragility of piping Tee-joint from proposed-scaled ground motions: nonlinear FE analysis versus probabilistic analysis 104

PART I: INTRODUCTION

1. Introduction

Historically, seismic analysis and design of buildings has received considerably much greater attention from researchers. In recent years, failure of nonstructural components during earthquakes has resulted in significantly high economic losses. Some of these failures have also resulted in injuries and in rare cases loss of life. In critical facilities such as hospitals, power plants, and school buildings, nonstructural components such as piping systems must remain operational or functional after an earthquake. It has been reported that economic losses due to the failures of nonstructural components has been much more considerable than those due to failure of structural systems in many recent major earthquake disasters (Fleming, 1998; Kircher, 2003; Soong and Garcia, 2003). It has also been observed that the seismic fragility of nonstructural components could be much higher than that of structural components (Ju, 2012). Therefore, research is needed in the area of seismic design and analysis of nonstructural systems such as piping particularly with an emphasis on performance-based seismic fragility evaluation.

Many articles have described the severity of past earthquake damage with respect to nonstructural components. For example, during the 1971 San Fernando Earthquake, 4 of the 11 major medical facilities in the area had extensive damage to nonstructural systems (Wasilewski, 1998) and during the 1994 Northridge Earthquake, 3 hospital buildings in the area were shut down and 915 patients evacuated. The Olive View Hospital which was retrofitted for withstanding earthquake forces after the 1971 San Fernando Earthquake was also shut down because of damage to nonstructural components (Ayres, 1998). The economic loss due to the failure of nonstructural components was more than 50% of total loss.

However, limited research has been conducted on seismic design of nonstructural components such as piping systems. Therefore, the performance of nonstructural components has emerged as an important area of research in recent years.

The ATC-58 project has proposed tools and guidelines for performance-based seismic design and performance assessment. These are based on probabilistic theories with the consideration of uncertainty and variability of seismic hazard, structural/nonstructural responses, damage states, and both economic and casualty losses (ATC, 2008). The performance-based assessment requires scaling of recorded earthquake ground motions to conduct nonlinear response time history analysis. A key objective of the scaling procedure is to preserve the distribution (both the median and the dispersion) in the earthquake shaking for the selected characterization of the hazard to enable appropriate consideration of distribution in responses and demands for the structural and the non-structural systems. The advantage of using recorded earthquake records is that the original characteristics of individual records including the peaks and valleys in the response spectrum are retained.

This thesis focuses on reviewing several existing scaling methods and presents the results from a study that compares and contrasts the applicability of each individual widely used method as well as some of the recently proposed methods to nonstructural systems such as equipment and piping located inside a building. Unlike many of the recent studies in which the suitability of scaling methods are evaluated using nonlinear response analysis of single-degree-of-freedom (SDOF) systems, this study uses a real-life piping system (Ju, 2012). The failure criterion considered in the evaluation of piping fragility is based on the nonlinear behavior exhibited in the experimental studies (Tian, 2013; Ju, 2012).

In this thesis, we will propose a new method that maintains the advantages of existing methods and tries to eliminate their deficiencies. Not only the dynamic characteristics of an actual piping system will be considered in evaluating the ground motion scaling methods, the dynamic characteristics of supporting building will also be included as a factor in evaluating a good scaling approach. Seismic fragility on nonstructural piping systems is evaluated for each individual scaling method using the software package OpenSees. To more efficiently analyze the problem, this study also introduces a probabilistic approach as an alternative to multiple nonlinear time history analyses.

2. Objective

Traditional ground motion scaling method (single period scaling) doesn't capture the nature of the distribution (both the median and dispersion) in the earthquake shaking for the selected characterization of the hazard. Thereby, the seismic fragility assessment performed using conventional scaling approach is not acceptable. A key objective of this research is to compare and contrast the existing methods of scaling seismic ground motions for applications in the seismic fragility assessment of nonstructural systems. This would be achieved by a fragility evaluation of an actual piping system in a hospital. Depending upon the outcome of this study, a related objective is to propose a new or modified scaling procedure.

3. Proposed Research

The specific tasks needed to achieve the objectives of this study can be outlined as follows:

- Understand methodologies for developing seismic hazard, evaluating seismic fragility, and assessing seismic risk.
- Understand existing studies (Ju, 2012; Tadinada, 2012; Tian, 2013) that describe the seismic behavior of nonstructural piping systems. These studies focus on experimental tests, nonlinear behavior of threaded Tee-joints, characterization of limit state, and finite element based modeling.
- Select an actual piping system configuration that incorporates the experimental data on nonlinear behavior of the threaded T-joint. The particular piping system would be used for nonlinear analysis and fragility assessment. A related sub-task is to model the nonlinear model of the complete piping system using finite element software such as OpenSees (Mazzoni et al., 2006).
- Develop an understanding of the methodology for selection of ground motion records (deaggregation method) needed in a fragility assessment. Use the USGS online application tools as well as PEER NGA ground motion database for selecting ground motions and understand the fundamental basis of probabilistic seismic hazard assessment (PSHA).
- Select candidate methods of ground motion scaling for evaluating their acceptability with respect to fragility assessment in piping systems. The intent is to select some of

the widely used methods such as those recommended by codes and standards (IBC, 2012) and some of the recently proposed methods.

- Use the dynamic characteristics of the actual piping system and a typical building on which it might be supported to evaluate the applicability of each scaling method. More specifically, evaluate if a scaling method appropriately considers multiple periods because of significant contribution of higher order modes.
- Evaluate if a scaling method is appropriate in the large period range (representative of a building period) as well as in the small period range (representative of piping system modes).
- Evaluate if a scaling method appropriately considers the dispersion of spectral accelerations that is consistent with target values as given by the attenuation relationship.
- If none of the existing methods are found to appropriately address the needs of fragility assessment for nonstructural systems, propose a new method that overcomes the limitations of existing methods.

4. Organization

This thesis has been divided into three major parts. Part I gives the introduction and develops the need for conducting this research. It formulates the objectives of the proposed research and outlines several tasks are needed to conduct the proposed research. Part II of this thesis is a manuscript that is intended for submission and possible publication as a

journal article. This part provides the complete details of the research including the description background literature, key observations made in the research, the complete results, proposed methods, and the key conclusions. Part III of this thesis presents the detailed summary and conclusions of this research. This part also provides recommendations of future research in this area.

REFERENCES

Applied Technology Council (ATC). (2008). “Guidelines for seismic performance assessment of buildings.” ATC-58 50% Draft, ATC, Red-wood City, CA.

Ayres, J. M., & Phillips, R. J. (1998). “Water damage in hospitals resulting from the Northridge earthquake”. TRANSACTIONS-AMERICAN SOCIETY OF HEATING REFRIGERATING AND AIR CONDITIONING ENGINEERS, 104, 1286-1296.

Fleming, R. P. (1998). “Analysis of fire Sprinkler system performance in the Northridge Earthquake”. National Institute of Standards and Technology, Building and Fire Research Laboratory

International Code Consortium, “International Building Code (IBC) 2012,” 2012.

Ju, B. S. (2012). “Seismic Fragility of Piping System”. North Carolina State University

Kircher, C.A. (2003), “It Makes Dollars and Sense to Improve Nonstructural System Performance,” Proc. ATC 29-2 Seminar on Seismic Design, Performance, and Retrofit of Nonstructural Components in Critical Facilities, Newport Beach, CA, October 23-24, 2003.

Mazzoni, S., McKenna, F., Scott, M. H., & Fenves, G. L. (2006). “OpenSees command language manual”. Pacific Earthquake Engineering Research (PEER) Center.

Soong, T. T., & Lopez Garcia, D. (2003). Seismic vulnerability and protection of nonstructural components. In Proc. The Joint NCREE/JRC workshop on International collaboration on earthquake disaster mitigation research.

Tadinada, S. K. (2012). “A Bayesian Framework for Probabilistic Seismic Fragility Assessment of Structures”. North Carolina State University.

Tian, Y. (2013). “Experimental seismic study of pressurized fire sprinkler piping subsystems”. State University of New York at Buffalo.

Wasilewski, R. J. (1998). “Seismic restraints for piping systems”.

PART II: SCALING OF EARTHQUAKE GROUND MOTIONS FOR FRAGILITY ANALYSIS OF PIPING SYSTEMS

1. Introduction

The ATC-58 project has proposed tools and guidelines for performance-based seismic design and assessment. These are based on probabilistic theories for consideration of uncertainty and variability of seismic hazard, structural/nonstructural responses, damage states, economic loss and life safety (ATC, 2008). The performance-based assessment requires scaling of recorded earthquake ground motions to conduct nonlinear response time history analysis. A key objective of the scaling procedure is to preserve the distribution (both the median and the dispersion) in the earthquake shaking for the selected characterization of the hazard to enable appropriate consideration of distribution in responses and demands for the structural and the non-structural systems. The advantage of using recorded earthquake records is that the original characteristics of individual records including the peaks and valleys in the response spectrum are retained. IBC (2012) recommends that a minimum of seven ground motions records be considered in order to ensure that the response is not dominated by the peaks and valleys of a single record. Several different scaling procedures have been proposed and evaluated over the past decade or more (Shome and Cornell, 1998 May; Bazzurro and Luco, 2006 April; Huang et al., 2009; Baker, 2010). In almost all cases, suitability of these scaling methods has been evaluated by application to structural systems particularly buildings. Studies that evaluate suitability of these methods to nonstructural systems are very limited. This paper presents the results from a study that compares and contrasts the applicability of a couple of widely used scaling methods as well as a couple of the recently proposed methods to nonstructural systems such as equipment and piping located inside a building. Unlike many of the recent studies in which the suitability of scaling

methods are evaluated using nonlinear response analysis of single-degree-of-freedom (SDOF) systems, this study uses a real-life piping system (Ju, 2012). The failure criterion considered in the evaluation of piping fragility is based on the nonlinear behavior exhibited in the experimental studies and ASME code requirements (Tian et al., 2012; Ju 2012; Tian 2013).

Given a suite of earthquake records, "scaling" is defined as the procedure of applying a scale factor to each of individual record that increases or decreases its amplitude. The scale factor can be determined from one of the several methods and yet the primary objective of each method is same, i.e. the average spectral acceleration of the scaled earthquake records does not fall below a target design response spectrum in the period range of $0.2T_1$ to $1.5T_1$ where T_1 is the fundamental period of the structure (IBC, 2012; Baker, 2010). The design spectrum, as specified in various building codes, typically corresponds to a uniform hazard spectrum (UHS). It has been widely noted that the code based procedures were not developed for performance-based assessment and therefore do not meet most of its objectives. One of the reasons for differences cited in the literature relates to conservative nonlinear response of structures when UHS is used to represent the spectral shape for long return-period earthquake shaking (Cornell and Baker, 2006). It has also been shown that for highly nonlinear framing systems, the spectrally matched artificial records can result in unconservative displacement demands when compared to using the recorded ground motions (Bazzurro and Luco, 2006; Huang et al., 2009). Probabilistic seismic hazard analysis (PSHA) to characterize earthquake hazard is now a widely followed practice (Field, 2005). The selection of a suite of records is typically based on seismic hazard deaggregation, namely, similarities in site characteristics, magnitude, distance, and return periods. A key step in the PSHA relates to the

characterization of dispersion in seismic shaking by an attenuation relationship which is used to evaluate the median and logarithmic standard deviation of the spectral acceleration at different periods (Abrahamson et al., 1997). Significant discussion in recent years has focused on the relationship between spectral shape and randomness in ground-motion. This relationship is represented in terms of an index referred to by epsilon (ε) and is defined as the number of logarithmic standard deviations by which the underlying logarithmic spectral acceleration deviates from the median value (Baker, 2010). As mentioned above, the median and the logarithmic standard deviation in spectral acceleration needed in the evaluation of epsilon are obtained from the attenuation relationships. Baker (2010) recommends the concept of conditional mean spectra (CMS) which has an added advantage in the sense that the correlation between epsilons at different periods is considered to account for the effect of spectral shape.

In this study, we will compare and contrast four different methods considered in the various studies mentioned above. These are: (i) scaling to match the target spectral acceleration at a single period which is usually the fundamental period of the structure as explained in Shome and Cornell (1998), (ii) weighted scaling (or scaling in a range of periods) as explained in Baker (2010), (iii) scaling by a factor that is geometric mean over a set of periods as explained in Huang et al. (2009), and (iv) distribution scaling as described in Huang et al. (2009). The various aspects that need to be considered for comparing these methods, in the context of nonstructural system response evaluation, are described in detail in the next section.

2. Significance of Nonstructural Systems and Their Characteristics

In critical facilities such as hospitals and data centers, nonstructural components must remain operational or functional after an earthquake. Nonstructural components for maintaining the operation of the buildings are defined as architectural components, piping systems, mechanical and electrical equipment, and building contents. In recent years, the economic loss due to failures of nonstructural components has been much more considerable than that due to failure of structural systems in almost all seismic events (Ayres and Philips, 1998; Wasilewski, 1998). It has been observed that the seismic fragility of nonstructural components is much higher than that of structural components (Fleming, 1998). In some cases, the failure of nonstructural components has also resulted in injuries and loss of life.

Nonstructural damage, especially in hospital buildings, has dominated the overall economic losses during the past earthquakes. For example, during the 1971 San Fernando Earthquake, 4 of the 11 major medical facilities in the area had extensive damage to nonstructural systems (Wasilewski, 1998) and during the 1994 Northridge Earthquake, 3 hospital buildings in the area were shut down and 915 patients evacuated. The Olive View Hospital which was retrofitted for withstanding earthquake forces after the 1971 San Fernando Earthquake was also shut down for a week because of damage to nonstructural components (Ayres and Philips, 1998). The economic loss due to failure of nonstructural components was more than 50% of total loss. According to Fleming (1998), many instances of damage to sprinkler piping system in hospital buildings were observed during the Northridge Earthquake. Improvement in the performance of nonstructural components has

emerged as a key area of research in recent years. ATC-58 (2008) presents a methodology for performance based of nonstructural systems.

Very limited studies have been conducted on the experimental behavior as well as fragility assessment of nonstructural systems and in particular piping systems. Laboratory experiments on threaded piping connections particularly T-joints were conducted by Tian (2013). These tests evaluated the monotonic and cyclic moment-rotation behavior of the threaded joints and identified key rotations for "first leakage" at the joint. This test data was used by Ju (2012) to develop computational models that reconciled well with test data and also provided a basis for specifying a generic limit definition of performance criterion or limit-state. These nonlinear models were then incorporated in an actual fire-sprinkler piping system model to evaluate piping fragility. Ju (2012) also evaluated the influence of dynamic interaction between piping system and supporting building on the piping fragility. Later, Tian (2013) conducted large-scale experiments on a fire-sprinkler branch piping system that consisted of configurations on two floors connected by a riser as well as connection of sprinkler heads with ceiling tiles. Ryu (2013) conducted numerical modeling of this system that reconciled well with the experimental results and subsequently calculated piping fragility of this system. All these fragility analyses used a suite of 21 ground motion records which were amplitude scaled to the same value of peak ground acceleration (PGA). Therefore, these results cannot be used directly to compare and contrast the relative suitability of various scaling methods.

As identified in previous studies (Ju, 2012), the behavior of nonstructural systems such as piping or equipment can be significantly different from that of structural systems in the sense that fundamental mode is not the significant mode in most cases. Depending upon the performance criterion or limit-state, higher order modes can play a significant role in the overall response evaluation. In many cases, the higher order modes that govern the performance are actually local modes. The behavior of nonstructural systems can also be highly dependent upon its interaction with the building/structural system that they are attached to. The effect of interaction is greatest between a significant mode of the nonstructural system and a building mode whose frequency is closest to significant mode of nonstructural system. In a nonlinear system, not only the interacting modes play a critical role but the fundamental mode of the building can also contribute significantly as any nonlinearity in the building results in significant changes in the earthquake motion at the location of nonstructural system. In general, the building's fundamental mode period is much longer than the fundamental period of the nonstructural systems. This together with the significance of higher modes imposes greater constraints on the process of scaling earthquake ground motions. These constraints and their influence on the fragility assessment of nonstructural systems is illustrated in detail in this paper.

Wood (2012) conducted a detailed study on selecting an appropriate scaling method in the performance evaluation of partition walls in buildings. He considered the effect of higher modes beyond what has been considered in other studied by considering building modes and recommend the use of a method that considers a weighted scaling method over a

range of periods. Selection of a range of periods in this method is based on acceptable mass participation among the first few modes which in case of buildings are typically the first two modes. While this study is a very valuable contribution towards the inclusion of higher modes effect in scaling methodology, an additional objective that needs to be considered in the selection of scaled ground motions relates to the dispersion of the scaled ground motions that needs to be consistent with the probabilistic seismic hazard assessment. It is precisely for this reason that we consider distribution-scaling method, not considered in Wood (2012), as one of the available methods in this study.

3. Piping System Configuration, Limit-State, and Dynamic Characteristics

The piping system configuration considered in this study is shown in Figure 1 and is the same system described in Ju (2012). The piping system, originally designed as per NFPA-13 (2007) and SMACNA (2003), is selected from a hospital building in California. This piping system was made up of 2, 3, and 4 inch diameter schedule 40 black iron pipe and the system is braced by transverse/longitudinal hangers and anchors at the ends of the pipes. Tian et al., (2012) conducted several laboratory tests on threaded T-joint for both monotonic and cyclic loadings. This study considered several types of piping materials and several dimensions of piping components but only the Black Iron threaded piping Tee-joint with 2 inch diameter is considered in this study. The test data consisted of force-displacement as well as the moment-rotation relationships for both monotonic and cyclic loading cases. We consider the nonlinear relationship for only the cyclic case and incorporate the reconciled

finite element model for the nonlinear T-joint in the piping system model for evaluating the system-level fragility as described in detail in Ju (2012).

The first step of system-level fragility analysis lies in the characterization of the failure limit-state. The limit-state is representative of a formal criterion corresponding to the observed failure or damage. As described in detail in Ryu (2013),"First Leakage" failure rotations from monotonic tests were larger than these observed in cyclic tests. Therefore, rotations at T-joint connections as observed from the cyclic tests can be a good engineering demand parameter to characterize the limit-state corresponding to the first-leakage instance. While the test data provides a good insight into the absolute values of rotations corresponding to first-leakage instance for each pipe diameter, the absolute values are likely to change significantly due to changes in material and/or geometrical properties of the threaded T-joint. Therefore, it is necessary to characterize the performance of the T-joint using a limit-state that can represent the behavior in a generalized form. Ryu (2013) compares the experimental results with the criterion that forms the basis of design guidelines specified in the ASME Boiler & Pressure Vessel Code (ASME 2007) which specifies the limit load criterion based on preventing the gross plastic deformation and large displacement of ductile materials. Using the same methodology, the criterion in this study is defined as limit rotation corresponding to the collapse moment in terms of performance characterization. Figure 2 shows the moment corresponding to the intersection of the moment-rotation curve and a collapse limit line such that $tan\,\phi = 2tan\,\theta$ relative to the ordinate. Angle θ is defined as the initial slope of the moment-rotation curve with respect to the moment-axis. In the moment-rotation curve, moment values on ordinate tend to be much bigger than the

rotation values on abscissa, which makes the angle θ much smaller. For the purpose of application, the angle can be assumed as $\phi = 2\theta$. Ryu (2013) used this criterion to define failure in terms of "First Leakage" in 2 inch black iron threaded, 1 inch black iron treaded and 4 inch black iron grooved fit T-joint piping connections. The safety demand against “leakage” is the primary objective in a pipe-joint connection of the types encountered in hospital and office building piping systems. Figure 3 shows that this criterion gives a good prediction of the limit for the 2 inch black iron schedule 40 pipes with treaded joints considered in this study.

The representative piping system considered in this study is an actual fire sprinkler piping system taken from a hospital in California. The hospital piping system shown in Figure 4 consists of main piping runs along 4 sections with a total of 64 branches in all. The main runs of the piping system comprise of 2-inch and 4-inch diameter pipes whereas the branches comprise of pipes with diameters smaller than those of the main pipe runs. This system is supported by unbraced single hangers, transverse braced hangers and longitudinal braced hangers at various locations. The details of actual support locations are not provided in this paper for brevity. There are 4 anchors at the ends of the four main piping system runs. Since all the supports of the piping system are connected to the same ceiling, they all experience the same earthquake input. The natural frequencies for this piping system for the first 20 modes are given in Table 1. Ideally, the earthquake input exhibited by the piping through its supports is an amplified earthquake motion filtered through the building to which the piping is connected. Typically, the amplification is higher on higher floors and the filtering changes the characteristic of earthquake motion. The degree of amplification and

nature of modification due to filtering in a time history is different for different buildings which cannot be generalized. Therefore in this study, we consider free-field earthquake ground motions applied directly to piping supports. This situation is representative of a piping system in low rise buildings (less than 4 or 5 stories tall). The effect of building's own characteristics and its interaction with the piping system introduces additional complexities. Ju (2012) and Ryu (2013) considered different buildings to evaluate piping fragilities by considering interactions with building systems. For brevity and a focused discussion on scaling methods, we do not consider building model in the fragility analysis in this study. Yet, we evaluate and discuss the appropriateness of the scaling methods with respect to the fundamental building period of a 20-story building considered by Ju (2012). Therefore, the fragility results presented in this paper are relatively more valuable for piping systems in low rise buildings including hospitals, office spaces, hotels, schools, etc.

Unlike a building structural system whose response is contained primarily in the fundamental mode which is also the global structural mode, the response of a piping system is highly dependent upon (1) higher order modes, and (2) piping modes that contribute significantly to the failure limit-state which are a local mode and not a global piping mode. Figure 5 gives several mode shapes (global fundamental mode, first local mode, and second local mode) of the piping system. It can be observed that the 1st mode shape associated with the fundamental period of the system does not influence the response at the location the Tee-joint where the "first-leakage" failure is observed. The 3rd mode of the piping system (T_{p3}) induces the vibration of the Tee-joint and has potential to fail the piping system. Several modes may contribute to the failure because there are multiple local modes that affect the

particular T-joint of interest. To illustrate this point further, Figure 5 shows the 9th piping mode shape (T_{p9}) which also influences the response at the T-joint of interest. These characteristics can play a significant role in earthquake ground motion scaling philosophy, and the corresponding results from a fragility analysis.

4. Selection of Earthquake Ground Motions

The Uniform Hazard Spectrum (UHS) is constructed by enveloping the spectral amplitudes at all periods that are exceeded with certain probability (2%, 5%, 10%, etc.) in 50 years. In engineering practice, UHS is developed from hazard curves corresponding to certain probability of exceedance and is affected by site conditions (Baker, 2010). In continental United States, UHS is available in United States Geological Survey (USGS) official website, it can be found at http://geohazards.usgs.gov/hazardtool/application.php (USGS, 2008a)

Apart from the design spectrum defined in codes like ASCE7-05, site-specific UHS is also used as target spectrum for ground motion scaling in many cases. The site of interest in this research is located in the city of Charter Oaks (longitude 117.856 W, latitude 34.102) in southern California. The site is selected because of its high rate of seismic activity and also because Wood (2012) considered it in a similar study on fragility of partitions. The target acceleration response spectrum used for ground motion scaling is the site specific UHS generated using the USGS procedure with 2% of exceedance in 50 years and site class C

(shear wave velocity ranges from 365m/s to 760m/s in the upper 30 m). Figure 6 gives the UHS curve at site of interest.

The ground motions selected must be consistent with site specific PSHA. A seismic hazard analysis corresponding to a probability of exceedance of 2% in 50 years is evaluated utilizing 2002 version of USGS National Seismic Hazards Mapping Project which gives the estimated magnitude (*M*) and source to site distance (*R*) bins at the site of interest (USGS, 2008b, Figure 7, Table 2)

The PSHA was conducted at PGA level for deaggregation analysis. Table 2 gives the statistical results indicating that 100% of the hazard is associated with sources less than or equal to 20 km, and 84.457% of the hazard is associated with sources less than or equal to 10 km of the site. In addition, the deaggregation also implies that 77.73% of the hazard is associated with magnitudes larger than 6.5, and 53.68% of the hazard is associated with the magnitude range of 6.5-7.0. The up-to-date deaggregation tool available is the 2008 version which would give us slightly different distributions of *M* and *R*, but such difference would not influence the basic analytical procedures in ground motion selection. Since deaggregation gives the realistic geological and seismological features at the site of interest, the earthquake events and corresponding ground motions selected for nonlinear finite element analysis should reflect such characteristics.

The seismic hazard deaggregation generated above is the most important criterion that guides the selection of ground motion records. In addition, other criteria have been

suggested that selected ground motion must comply with (Wood, 2012; Bommer and Acevedo, 2004; Haselton's Group I, 2009):

- Ground motion records should be taken from strong motion instruments setup in the free field,
- Ground motion records should conform to the soil conditions of the site of interest: site class C defined in ASCE7-05 (IBC, 2012) with shear wave velocity in the upper 30 m ranging from 365m/s to 760m/s,
- Ground motion records should be compatible with the source focal mechanisms and tectonic regime expected at the site,
- Magnitude-distance (*M*, *R*) of selected ground motion records should reflect the features of results of the deaggregation analysis from site-specific PSHA.

A total of 21 ground motions chosen following above-mentioned screening standard are organized and listed in Table 3 and satisfy the requirements related to free-field, site classification, and focal mechanism. Statistics of these records also indicate that 21 out 21 (100%) motions are associated with sources within 20 km or less, and 18 out of 21 (85.71%) motions are associated with sources within 10 km of the site. 16 out of 21 (76.19%) motions are associated with magnitudes larger than 6.5, and 11 out of 21 (52.38%) motions are associated with magnitude in the range of 6.5 to 7.0. Selected earthquake records are compatible with site-specific deaggregation results given above.

It is observed from Figure 8 that the shape of median (50% exceedance) response spectrum of the unscaled ground motions is similar to median predicted UHS (and of course

2% UHS), but Figure 9 indicates that logarithmic standard deviation (β) doesn't match well with target and is thereby unable to preserve the distribution (median and β) of seismic hazard. The lack of a good match of β verifies that rigorous ground motion selection mechanism cannot solve the problem by itself and the scaling methods are needed to ensure that both the acceleration response spectrum and β match well with corresponding targets.

5. Methods for Scaling Ground Motions

As mentioned earlier, we evaluate the suitability of four different scaling methods in the fragility assessment of piping systems. A general description of each of these methods is presented below.

5.1. Single Period Scaling Method (Sa(T_i) Scaling Method)

In this method, the earthquake records are scaled in their amplitudes to match a target spectral acceleration at a single period of interest (Shome and Cornell, 1998 May). The period of interest is typically taken as the fundamental period of the structure with a premise that the fundamental period is the most critical period in evaluating the response of buildings and other structures. The target response spectrum acceleration usually corresponds to that from the uniform hazard spectrum (UHS) at the period of interest. Mathematically, each ground motion is multiplied by a scale factor SF_i:

$$SF_i = \frac{SA_{UHS}(\mathrm{T}^*)}{SA_i(\mathrm{T}^*)} \tag{1}$$

where SA_{UHS} is the spectral acceleration from UHS and SA_i the spectral acceleration for i^{th} record period T^*. Figure 10 shows the selected 21 ground motions scaled to match target 2% UHS using single period scaling method at the period 0.315s. The figure displays a "pinch" (Baker, 2010) at scaling period T=0.315s (first local mode) because single period based scaling guarantees that spectral accelerations from different records are all equal at that period. At periods other than T^*, this method introduces large scatter in the spectral accelerations.

5.2. Multiple Period Scaling Method ("Range" Scaling Method)

In this method, each individual ground motion is scaled such that the resulting spectrum is approximately equal to the target spectrum over a range of periods (Baker, 2010). Mathematically, scaling procedure involves multiplying each ground motion by the following scale factor SF_i.

$$SF_i = \frac{\sum_{i=1}^{n} SA_{UHS}(\mathrm{T}^*)}{\sum_{i}^{n} SA_i(\mathrm{T}^*)} \tag{2}$$

Where n is the total number of scaling points used in the range of $0.2T_1$ to $1.5T_1$. Figure 11 gives the scaled selected 21 ground motion spectra to match the target 2% UHS over a specified range of periods. As seen in this figure, the "pinching" behavior is not observed and each individual spectrum is closer to the UHS over the entire range of periods of interest.

5.3. Geometric Mean Scaling Method

A scaling method similar to "range" scaling that operates over a period range is termed as Geometric Mean Scaling Method. It was developed for offshore oil industry and utilized in the SAC Steel Project (1997). The method involves multiplying the entire suite of ground motions by a single factor such that the sum of the squared errors between the target UHS and the geometric mean of spectral ordinates for each ground motion will be minimized. The target periods are selected by users (Huang et al., 2009). The scale factor associated with the minimum squared errors is usually obtained from iterative calculation. This method preserves the spectral acceleration shape and original dispersion of unscaled ground motions. A good match is determined by careful ground motion selection mechanism; meaningful results are obtained when both the median spectrum acceleration and dispersion of ground motions match well with corresponding targets are guaranteed. However, ensuring both requirements in most cases is quite impractical and sometimes not possible. The plot of geomean scaled case is shown in Figure 12. It must be noted that the β plot is the same as that in the unscaled case shown in Figure 9.

5.4. Distribution Scaling Method

As a key limitation, the scaling methods described above cannot account for the dispersion in seismic shaking in a manner that is consistent the dispersion specified by the attenuation relationship for the median and logarithmic standard deviation of the spectral acceleration at different periods (Abrahamson, 1997). Distribution scaling method (D-Scaling Method) is a novel approach to improve this deficiency. Starting with the

fundamental assumption that the spectral accelerations are lognormally distributed at a given period T_i, D-Scaling method scales different ground motion records to different spectral ordinates such that the median θ and dispersion β are consistent with those specified by the attenuation relationship (Huang et al., 2009).

The target UHS in this research is computed from PSHA, which envelopes spectral amplitudes at all periods with 2% probability of exceedance in 50 years. PSHA also gives deaggregation information (mean causal magnitude *M*, mean causal distance *R*, and epsilon value of the "median" predicted UHS) of earthquake events most likely to occur for the target spectral acceleration at given period. The "median" predicted UHS constructed using this method is smaller than UHS, as can be seen from Figure 13. The "median" predicted UHS gives the median θ and dispersion β necessary to perform D-Scaling method.

To illustrate the method, let us consider an example case such that θ=0.2g, β=0.3 at period T_i and a total of 5 ground motions, n = 5, are considered. The probability density function (PDF) and cumulative distribution function (CDF) associated with given condition is shown in Figure 14. The CDF is now divided into 5 regions with each one equal probability of 0.2 (e.g. 0 to 0.2, 0.2 to 0.4…0.8 to 1), and the spectral ordinate for scaling is at the midpoint of each region in the CDF. Each ordinate x_i can be calculated from the following equation:

$$x_i = \theta \cdot e^{\beta \cdot \Phi^{-1}(\mathrm{P}_i)} \tag{3}$$

Where,

Φ^{-1} = inverse standardized normal cumulative density function (CDF);

P_i = cumulative probability at midpoint for i^{th} region and equals (i-0.5)/n

x_1 is defined as the spectral acceleration corresponding to middle point of 1st 20% region in CDF, which corresponding to $P(\mathrm{X} < \mathrm{x}_1) = 0.2$, and x_1 could be determined from Equation (3):

$$x_1 = 0.2 \bullet e^{0.3 \bullet \Phi^{-1}(0.1)} = 0.2 \bullet e^{0.3 \bullet (-1.285)} = 0.136$$

x_i at other regions could also be calculated in similar method, and x_1 to x_5 comprise of the 5 spectral ordinates (0.136g, 0.171g, 0.2g, 0.234g, 0.294g) corresponding to 0.1, 0.3, 0.5, 0.7 and 0.9 probability values in CDF at period *Ti*. These values are then used for scaling the ground motions (Huang et al., 2009). The procedure of D-Scaling method can be summarized as:

(1) For a given period of interest T_i, produce n (the number of total available ground motion records) target spectral acceleration ordinates x_i to x_n using Equation (3) based on the median and logarithmic standard deviation obtained from site specific attenuation relationship,

(2) Calculate the spectral acceleration value for each ground motion at the period of T_i,

(3) Scale *n* ground motion to corresponding target ordinates.

6. Assessment of Scaling Methods

In this section, we use the 21 ground motions selected using the procedure described in section-4 above to evaluate the applicability of each of the four scaling methods in fragility assessment of piping systems. The median UHS obtained from unscaled ground motions is compared to the target UHS in Figure 8. The logarithmic standard deviation β over the entire period range for the unscaled motions is also compared with the target β in Figure 9. The target response spectrum in this figure is the 2% UHS in the city of Charter Oaks as mentioned in ground motion selection procedure. The target β refers to that recommended in Abrahamson, (1997). Furthermore, it must be noted that the critical mode of our piping system is not the fundamental piping mode but a local mode which is the 3rd mode of the piping system with period T_{p3}, the second critical mode for the failure location is the 9th piping system mode with period T_{p9}, and the fundamental mode of the 20 story building considered in Ju (2012) has a period denoted by T_{b1}which equals to 2.07s. Section 3 discusses the values and significance of these critical modes in detail.

6.1. Single Period Scaling

We evaluated three different spectra and the corresponding logarithmic standard deviations by scaling the 21 ground motions using Equation (1) at these three different distinct periods. Figure 10 shows the comparison for scaling at T_{p3}, Figure 15 that for scaling at T_{p9}, and Figure 16 that for scaling at T_{b1}. In each of these 3 cases, a comparison of the individual spectra for the 21 ground motions with the scaled spectrum curve would display the feature of "pinch" (Baker, 2010) at scaling period of interest because single period based

scaling ensures that spectral accelerations from each individual record are identical at the period of scaling. This particular characteristic of the single period based scaling method makes it inconsistent for application to the case of nonstructural systems such as piping where multiple modes of both piping and building contribute significantly to the response.

A very interesting observation in Figure 10b, 15b and 16c relates to the nature of variation in the logarithmic standard deviation of scaled ground motions. As seen in these figures, the logarithmic standard deviation becomes exactly equal to zero at the particular period selected for scaling in the Equation (1). This is so because of the inherent nature of Equation (1) that makes the spectral acceleration for all individual ground motions exactly equal to that from the UHS at the specific period selected for scaling thereby making $\beta = 0$ at that particular period. Consequently, this method becomes inappropriate for consideration in the fragility assessment of any structural system even if the response is contained primarily in one mode. To explain this outcome further, let us consider an SDOF system that remains linear for the spectral acceleration given by UHS at its fundamental period. The response of this system will be "identical" from all the 21 scaled ground motions and there would be no variation at all. The very basis of using a suite of several scaled ground motions in a fragility assessment is related to consideration of uncertainty in the earthquake response of a structure due to varying ground motions. If the structure experiences nonlinear behavior, the softening would increase the effective period at any given snapshot in the analysis and the logarithmic standard deviation of the scaled motions will no longer be zero but it would still be much less

than the target values as seen from the variation in Figure 10b, 15b and 16c unless the period changes significantly.

6.2. Multiple Period Scaling Method ("Range" Scaling Method)

We use Equation (2) to evaluate the scaling factor for each ground motion. As discussed in section 5.3, a period range of $0.2T_{p3}$ to $1.5T_{p3}$ is considered and the number of periods *n* considered in the summation over this range is taken as 42. These periods are listed in Table 4. As one can infer, the results are somewhat sensitive to the number of periods selected in this method. Figure 11a compares the scaled median spectrum with the target 2% UHS. A key difference with respect to single periods scaling is that unlike single periods scaling case, no "pinch" is observed in this figure. The comparison of logarithmic standard deviation of scaled spectral accelerations shows that the problem of β = 0 does not exist anymore. Clearly, the logarithmic standard deviation for the selected ground motions has a relatively better trend compared to the single period based scaling method and represents a significant improvement. However, it is likely to be considered inappropriate because the β is less than the target values in the lower period range (periods corresponding to significant piping modes). The β values are greater than the target values in the higher period range (corresponding to building mode periods) but that is likely to be acceptable because the β values lie on the conservative side in this range of periods.

6.3. Geometric Mean Scaling Method

As mentioned earlier, this method was developed with an intent to preserve the spectral shape and the original dispersion of unscaled ground motions. It is believed that a

good match can be obtained by a careful selection of ground motions. Figure 12a compares the median spectra for the scaled ground motion by using this method with the median UHS. This figure also gives the comparison of logarithmic standard deviation which is much higher than the target values in the entire range of periods. In fact, this variation is almost identical to the corresponding variation seen in Figure 12b that shows the variation for unscaled ground motions. Consequently, this approach is not likely to be suitable for fragility assessments.

6.4. Distribution Scaling Method (D-Scaling Method)

This method takes the results of PSHA into consideration which captures not only the median but also the dispersion of spectral accelerations in the selected hazard at a period of interest T_i. In addition, probabilistic theory is utilized to distribute selected ground motions since the target median spectral acceleration and logarithmic standard deviation are known. The 21 unscaled motions were scaled in accordance with this method by considering the lognormal distribution of spectral accelerations at the critical piping period of interest T_{p3}. Figure 17 compares the scaled median and the logarithmic standard deviation plots with target values. As can be seen from this figure, this method is somehow similar to single period scaling, i.e. the distribution (both the median and logarithmic standard deviation) is preserved only at a single period. Therefore, this method overcomes the limitation associated with preserving the β values in a single period scaling method but the limitations related to preserving distribution at multiple periods of interest persists. Excessively high values of β associated with lower period values (corresponding to higher order piping modes) makes this

method less desirable. In the process of applying this method, we encountered an additional limitation that is described separately in the next section.

6.5. Non-Uniqueness of D-Scaling Method

In the course of this study, it was determined that unlike other scaling methods, the results obtained from D-Scaling method may change based on the ordering of the unscaled ground motions. As each individual ground motion is placed in a separate bin according to lognormal distribution, the scale factor for a specific record changes if it is placed in a different bin which in turn changes the overall results. An attempt is made in this section to evaluate the effect of this change further. To do so, the unscaled motions were ordered differently using three different criteria before applying the D-Scaling method. First, the records were ordered and distributed based on the Magnitude M of the earthquake event associated with them. The corresponding results for the median spectra and the logarithmic standard deviation are shown in Figure 18. We refer to this variation of the D-Scaling method by "Magnitude ordered D-Scaling" method. Second, the records were ordered and distributed based on the values of their respective unscaled values of Peak Ground Accelerations (PGA). We refer to this variation by "PGA ordered D-Scaling" method and the results obtained from this variation are shown in Figure 19. Finally, the records were ordered and distributed based on the values of their respective maximum spectral acceleration values. The results for this variation of the D-Scaling method referred to by "SA ordered D-Scaling" method are shown in Figure 20. As seen in these figures, the Magnitude ordered D-Scaling method shows significant improvements in the β values especially in the lower period region of interest

(corresponding to the higher order piping modes). The variations in β values for the PGA ordered D-Scaling and SA ordered D-Scaling methods are quite similar to those for the original case of no particular ordering in the D-Scaling. Despite the improvement seen in Figure 18 for the Magnitude ordered D-Scaling case, the method continues to exhibit the limitation mentioned earlier in the previous section that it is quite similar in nature to the single period scaling.

7. Piping Fragility for Different Scaling Methods

Seismic structural fragility is the probability of a structure to reach or exceed a specified limit state on condition of a given ground motion intensity parameter λ (λ could be PGA or spectral acceleration (Sa) at a certain period). The equation below gives the mathematical expression of seismic fragility:

$$P_f(\lambda) = \mathrm{P}[C - D \le 1 | \lambda] \tag{4}$$

Or

$$P_f(\lambda) = \mathrm{P}[\frac{C}{D} \le 1 | \lambda] \tag{5}$$

Where *C* represents the capacity that a structure can endure under seismic loads failure occurs in accordance with appropriate limit-state. *D* refers to the response demand on a structure at λ. Both, C and/or D, follow certain variation which is typically characterized by a probabilistic distribution (normal distribution, log normal distribution or other distributions), and they have to be evaluated by accounting for uncertainty associated with

capacity and demand variables for the structure (Tadinada, 2012). A fragility curve is intrinsically a cumulative distribution function (CDF) which describes the relationship between the ground motion intensity parameter λ (such as PGA or Sa) and the corresponding probability of failure P_f .

For this study, the limit-state for piping performance evaluation in accordance with the above mentioned equation can be written as:

$$P_f(\lambda) = \mathrm{P}[\theta \geq \theta_{\lim} \mid \lambda] \tag{6}$$

Where, $\theta_{\lim}$ is the limit state rotation or the rotation corresponding to the "first leakage" and is evaluated using the characterization given earlier in section 3 and illustrated in Figure 3. Test data from laboratory experiments on T-joints (Tian, 2013) is used to characterize the limit-state in this study. Each of the 21 ground motions is utilized to conduct nonlinear FE analysis of the complete piping system by incorporating the nonlinear moment-rotation relationship at the location of T-joints into the complete piping system mode. The equation for nonstructural seismic fragility can be further updated in the following form:

$$P_f(\lambda) = \frac{\sum_{i=1}^{N} (\theta_{i,\lambda} \geq \theta_{\lim} | \lambda)}{N} \tag{7}$$

Where,

$\theta_{i,\lambda}$ = The rotation from i^{th} ground motion at the level of λ ;

$\theta_{\lim}$ = Limit state rotation of Tee joint;

λ = Ground motion intensity parameter;

N = Number of earthquake ground motions

The seismic intensity parameter is characterized by the spectral acceleration at the period of a particular mode of interest. Three different periods are considered depending upon the period used in the scaling methods. These correspond to the 3rd piping mode T_{p3}, 9th piping mode $T_{p9,}$ and the fundamental building mode $T_{b1.}$

The seismic fragility curves for different ground motion scaling methods described in previous sections are shown in figure 21 to figure 29. These curves are smooth as they are plotted by considering the fragility model to be lognormally distributed just like in most of the previous studies (Tian et al., 2012; Ju 2012, Tian 2013). As seen in these figures, each individual curve appears to be quite different. It must be noted that the seismic intensity parameter used to plot each curve is different based on the particular scaling method used. Consequently, the relationship among the various curves is not directly apparent from these figures. An appropriate comparison of different curves would therefore require plotting each to the same value of seismic intensity parameter. Since the critical piping mode that is most critical in this study corresponds to period T_{p3}, the fragility curves are plotted in Figures 30 to 32 with respect to the median value of spectral acceleration Sa at T_{p3}. These modified fragility curves offer the following interesting observations:

- The median values of the fragility estimates corresponding to 0.5 (50%) probability of failure are almost identical or very close to each other irrespective of the scaling

method used. The reason for this behavior lies in the fundamental basis that each scaling method attempts to provide a good match of median spectra with the median UHS. The median spectral accelerations for different methods at T_{p3} are very close to each other and therefore the median fragility estimates are very close to each other.

- The fragility curve for single period scaling at T_{p3} is almost vertical indicating that there is no variation or uncertainty in the behavior. This is reflective of the fact that the logarithmic standard deviation for spectral acceleration at T_{p3} from this method is exactly equal to zero, as seen in Figure 10b and discussed earlier.
- One may argue that if $\beta = 0$ for this particular case of single period scaling then the fragility curve should be completely vertical. The answer lies in the fact that the period of the critical piping mode changes as the piping T-joint exhibits nonlinear behavior and causes a softening of the T-joint. This change in the period cause the β to exhibit a deviation from its zero value. The nature and degree of change in β would depend upon the degree of change in the period due to softening. In addition, the effect of higher order modes and their influence on failure at this location is also exhibited in the variation of β observed.
- The reasons for almost vertical nature of this curve provide an alternative option to understand and use this curve. Since all the scaled ground motions have almost identical median spectral acceleration on T_{p3} scale and $\beta = 0$ for single period scaling at T_{p3} while the only variation is due to different degree of nonlinearity exhibited by piping system in different earthquakes, this resulting β (although small) and the

median capacity of this curve is representative of the variation in piping's capacity *C*. Such a consideration forms the basis of a proposed fragility assessment method presented later in this study.

- Even though the median fragility estimates for different scaling methods are very close to each other, the curves vary significantly from each other due to differences in β values at period T_{p3} from each method. A higher the values of β results in a curve that is spread over a wider range of spectral accelerations.

8. Proposed Scaling Method

Discussion of results presented in the previous sections emphasizes that an accurate evaluation of fragility assessment in nonstructural systems requires an appropriate scaling method that gives close values of not only the median spectra with the corresponding median values of UHS but also the logarithmic standard deviation that is close to the target values in the entire period range of interest. It is also observed that none of the available methods are able to do satisfactorily for the case of piping system considered in this study. Therefore, a study of some alternative methods has resulted in the following proposed method for scaling earthquake ground motions.

The proposed method is built upon key strengths of the two existing methods and attempts to overcome their individual limitations. First, it utilizes the strength of D-Scaling method to allow appropriate and scientific consideration of logarithmic standard deviation. Second, it is built upon the strength of the geometric scaling method to account for

appropriate scaling at multiple periods. The proposed method is termed as "Geometric Mean based Magnitude ordered D-Scaling Method." The steps to achieve the desired scaling in this method can be enumerated as:

- Order the selected ground motions according to the Magnitude *M* associated with their respective earthquake event.
- Use D-Scaling method to evaluate the scaling factors at a desired period of interest
- Repeat the previous step at multiple periods in the entire range of interest.
- For each individual ground motion, combine the scaling factors at different periods into a single scaling factor by using the geometric mean.

Figure 33 shows the results obtained by scaling the 21 ground motions using this method. As seen in this figure, the median scaled spectrum matches well with the target median UHS and the scaled logarithmic standard deviation has a relatively much better match with the target values in the entire range of periods considered.

9. Proposed Method for Fragility Assessment

In this section, we use the fundamental probabilistic approach to develop and propose a fragility model. The proposed model is intended to reduce if not eliminate the variability in fragility assessment due to scaling methods. We start with the key observation made in section 7 about the fragility curve shown in Figure 30 and obtained from single period scaling method for critical piping mode T_{p3}. Let this curve represent the variation in the capacity of piping system. If C is defined as a logarithmically distributed capacity parameter,

the median failure spectral acceleration value (corresponding to 50% probability of failure) θ_C = 3.15g. Consider a range with an upper bound given by the median plus three logarithmic standard deviations and the lower bound given by the median minus three logarithmic standard deviations. This range accounts for 99.7% of the area under the distribution. These lower and upper bound values corresponding to fragility curve are 1.4g and 6.6g as is shown in Figure 30. A lognormal distribution then gives,

$$3.15g \cdot e^{3\beta_c} = 6.6g \tag{8}$$

$$3.15g \cdot e^{-3\beta_c} = 1.4g \tag{9}$$

These equations give $\beta_C = 0.28543$

Let the demand parameter D also follows lognormal distribution, i.e., $D \sim LN(\theta_D, \beta_D)$ in which θ_D is the median Sa value at T_{p3} and β_D is the logarithmic standard deviation at T_{p3} for any specific given ground motion scaling method. The failure criteria for the piping Tee-joint can be expressed as:

$$C < D \text{ or } \frac{C}{D} < 1 \tag{10}$$

Alternatively, we can define a lognormal distributed variable Z such that

$$Z = \frac{C}{D} \tag{11}$$

$$Z \sim LN(\theta_Z, \beta_Z) \tag{12}$$

$$Where\ \theta_Z = \frac{\theta_C}{\theta_D} \text{ and } \beta_Z = \sqrt{\beta_C{}^2 + \beta_D{}^2}$$

The fragility can then be expressed as:

$$P_f = P\ [\mathrm{Z} = \frac{C}{D} < 1] = \frac{\theta_C}{\theta_D} \cdot e^{\Phi^{-1}(\mathrm{P_i})\beta_Z} < 1 \tag{13}$$

The threshold value (failure criteria) is defined as:

$$\frac{\theta_C}{\theta_D} \cdot e^{\Phi^{-1}(\mathrm{Pi})\cdot\beta_Z} = 1 \tag{14}$$

And the probability of failure can be calculated from the equations below:

$$e^{\Phi^{-1}(\mathrm{P_i})\cdot\beta_Z} = \frac{\theta_D}{\theta_C} \tag{15}$$

$$\Phi^{-1}(\mathrm{P_i}) = \frac{\ln(\frac{\theta_D}{\theta_C})}{\beta_Z} \tag{16}$$

The lognormal standard distribution values can provide the probability of failure at any demand of interest. Seismic fragility curves for unscaled ground motions as well as each individual scaling method are plotted based on Equation (16) and are shown from figure 34 to figure 44 for some of the scaling methods considered in this research, respectively. The

results from those figures indicate a very good match with results conducted from the corresponding nonlinear FE analysis of the piping system.

10. Summary and Conclusions

The ATC-58 has proposed the need for performance based design and probabilistic methods for seismic risk mitigation. The performance-based seismic design requires the scaling of recorded earthquake ground motions to conduct nonlinear response time history analysis. A key objective of scaling procedure is to preserve the distribution (both the median and dispersion) in the earthquake shaking for the selected characterization of the hazard to capture behaviors in terms of response for both the structural and the non-structural systems.

The dynamic characteristics of nonstructural piping systems can be significantly different from that of structural systems in the sense that fundamental mode is not necessarily the significant mode in most cases. Higher order modes which are usually local modes play a significant role in the overall response evaluation and should be considered in ground motion scaling procedure. In addition, the behavior of nonstructural systems is highly dependent upon its interaction with the building/structural system that they are attached to.

This study presents results from a research that evaluates the suitability of various widely used ground motion scaling methods as well as some of the recently proposed methods. A total of 21 ground motions selected using seismic hazard deaggregation are utilized to conduct the nonlinear time-history response analysis. Seismic fragilities of piping

system are calculated for each individual scaling method for comparative purposes. The major conclusions of this research are summarized below:

- Single period scaling method is not appropriate in cases where multiple modes of the piping system or piping and building together contribute to the overall performance of the nonstructural systems such as piping.
- Even in those cases in which singe period is sufficient for response calculation, application of single period scaling method is impractical to use because the fundamental mode of nonstructural system is not necessarily the critical mode and a knowledge of the critical mode is needed to appropriately apply this method.
- Single period scaling method inherently results in a logarithmic standard deviation of zero which is incorrect in the fragility assessment of any structural system.
- Multiple period or "Range" based scaling method allows a better consideration of logarithmic standard deviation relative to the single period scaling method. However, it underestimates the values of logarithmic standard deviations at low periods which correspond to the higher order piping modes.
- The geometric mean based scaling method has the advantage of preserving the spectral shape. However, the logarithmic standard deviation from this method is much larger than that corresponding to the target values and is the same as the unscaled situation.
- The D-Scaling method provides a logically scientific approach to consideration of logarithmic standard deviation in the process of scaling ground motions. However, it

has the limitation of doing so at only single period. Consequently, it suffers from the same limitations as identified for the case of single period scaling method.

- The D-Scaling method is observed to suffer from non-uniqueness in the sense that the results are highly dependent upon the ordering of ground motions.
- The logarithmic standard deviations obtained from PGA ordered D-Scaling as well as SA ordered D-Scaling methods do not match well with the target values in the entire period range of interest.
- The proposed method which is based on Magnitude ordered D-Scaling with geometric mean gives a good match of logarithmic standard deviation with the target values in the entire period range of interest.
- The piping fragility curves vary significantly based on the scaling methods used.
- Most of the scaling methods result in fragility curves that have about the same median probability of failure but differ significantly in their dispersion. It is evident that the proposed scaling method gives the most appropriate fragility curve because it allows the best representation of logarithmic standard deviation.
- A simplified probabilistic approach is presented to evaluate fragility curve such that the fragility curves from various scaling methods are close to those obtained by the proposed scaling procedure.

REFERENCES

Abrahamson, N. A., & Silva, W. J. (1997). "Empirical response spectral attenuation relations for shallow crustal earthquakes". Seismological research letters, 68(1), 94-127.

ASME (2004), "Rule for Construction of Nuclear Facility Components", ASME Boiler and Pressure Vessel Code, Section III, American Society of Mechanical Engineers.

Applied Technology Council (ATC). (2008). "Guidelines for seismic performance assessment of buildings." ATC-58 50% Draft, ATC, Red-wood City, CA.

Ayres, J. M., & Phillips, R. J. (1998). "Water damage in hospitals resulting from the Northridge earthquake". TRANSACTIONS-AMERICAN SOCIETY OF HEATING REFRIGERATING AND AIR CONDITIONING ENGINEERS, 104, 1286-1296.

Bachman, R. and et al. (2004). "Engineering Demand Parameters for Nonstructural Components", ATC-58 Project Task Report, ATC, Redwood City, California.

Baker, J. W. (2010). "Conditional mean spectrum: Tool for ground-motion selection. Journal of Structural Engineering", 137(3), 322-331.

Baker, J. W., & Allin Cornell, C. (2006). "Spectral shape, epsilon and record selection". Earthquake Engineering & Structural Dynamics, 35(9), 1077-1095.

Bommer, J. J., & Acevedo, A. B. (2004). The use of real earthquake accelerograms as input to dynamic analysis. Journal of Earthquake Engineering, 8(S1), 43-91.

Bazzurro, P., & Luco, N. (2006, April). "Do scaled and spectrum-matched near-source records produce biased nonlinear structural responses". In Proceedings of the 8th US national conference on earthquake engineering, San Francisco, CA, Paper (No. 1029)

Field, E. H. (2005). Probabilistic seismic hazard analysis (PSHA): A primer.

Fleming, R. P. (1998). “Analysis of fire Sprinkler system performance in the Northridge Earthquake”. National Institute of Standards and Technology, Building and Fire Research Laboratory

Haselton, C.B. (Ed) (2009). “Evaluation of Ground Motion Selection and Modification Methods: Predicting Median Interstory Drift Response of Buildings.” PEER Technical Report 2009/01

Huang, Y. N., Whittaker, A. S., Luco, N., & Hamburger, R. O. (2009). “Scaling earthquake ground motions for performance-based assessment of buildings”. Journal of Structural Engineering, 137(3), 311-321.

International Code Consortium, “International Building Code (IBC) 2012,” 2012.

Ju, B. S. (2012). “Seismic Fragility of Piping System”. North Carolina State University

NFPA, A. (2007). 70-National Electrical Code. National Fire Protection Association, 1.

PEER-NGA (2009), Pacific Earthquake Engineering Research Center: NGA Database. http://geohazards.usgs.gov/hazardtool/application.php.

Ryu, Y. (2013). “Fragility of Piping Systems and Reliability of Piping Components”.

Shome, N., & Cornell, C. (1998, May). “Normalization and scaling accelerograms for nonlinear structural analysis”. In Sixth US National Conference on Earthquake Engineering, Seattle, WA.

SMACNA, A. (2003). Architectural Sheet Metal Manual. Sheet Metal and Air Conditioning Contractors' National Association.

Tadinada, S. K. (2012). “A Bayesian Framework for Probabilistic Seismic Fragility Assessment of Structures”. North Carolina State University.

Tian, Y. (2013). “Experimental seismic study of pressurized fire sprinkler piping subsystems”. State University of New York at Buffalo.

Tian, Y., Filiatrault, A., & Mosqueda, G. (2012). “Experimental seismic fragility of pressurized fire suppression sprinkler piping joints”. Earthquake Spectra.

United States Geological Survey (USGS). (2008a). Hazard Curve Application. USGS, Reston, Virginia. http://geohazards.usgs.gov/hazardtool/application.php.

United States Geological Survey (USGS). (2008b). 2002 Interactive Deaggregations. USGS, Reston, Virginia. http://eqint.cr.usgs.gov/deaggint/2002/.

Wasilewski, R. J. (1998). “Seismic restraints for piping systems”.

Wood, R. L. (2012). “Partition wall subsystem modeling and effect on the coupled building system response”. University of California, San Diego.

Table 1: First 20 period (sec) /frequencies (HZ) of the piping system

	p1	p2	p3	p4	p5
period	0.55	0.318	0.315	0.303	0.247
frequency	1.82	3.14	3.17	3.3	4.05
	p6	p7	p8	p9	p10
period	0.16	0.158	0.148	0.136	0.1339
frequency	6.25	6.33	6.76	7.35	7.47
	p11	p12	p13	p14	p15
period	0.1338	0.108	0.088	0.064	0.052
frequency	7.47	9.26	11.36	15.63	19.23
	p16	p17	p18	p19	p20
period	0.05	0.0462	0.0456	0.042	0.033
frequency	20	21.64	21.93	23.81	30.3

Table 2: Degaggregation bin details (% hazard)

M	source to site distance R (km)		sum
	0<R<10	10<R<20	
5.0-5.25	1.162	0	1.162
5.26-5.50	0.843	0	0.843
5.51-5.75	0.896	0	0.896
5.76-6.00	0.938	0.091	1.029
6.01-6.25	5.385	0.532	5.917
6.26-6.50	11.463	0.879	12.342
6.51-6.75	12.826	5.649	18.475
6.76-7.00	27.088	8.112	35.2
7.01-7.25	22.961	0.194	23.155
7.26-7.50	0.895	0	0.895
sum	84.457	15.457	99.914

Table 3: 21 selected ground motion records

	NGA #	Event	Year	Station	Focal mechanism	Site Class	Magnitude	Distance (km)
1	126	Gazli, USSR	1976	Karakyr	Unkown	C	6.8	4.7
2	496	Nahanni, Canada	1985	Site 2	Reverse	C	6.76	2.45
3	497	Nahanni, Canada	1985	Site 2	Reverse	C	6.76	5.1
4	802	Loma Prieta	1989	Saratoga - Aloha Ave	Reverse-Oblique	C	6.93	8.02
5	803	Loma Prieta	1989	Saratoga - W Valley Coll.	Reverse-Oblique	C	6.93	8.9
6	1052	Northridge-01	1994	Pacoima Kagel Canyon	Reverse	C	6.69	6.3
7	1086	Northridge-01	1994	Sylmar - Olive View Med FF	Reverse	C	6.69	3.5
8	1111	Kobe, Japan	1995	Nishi-Akashi	Strike-Slip	C	6.9	7.1
9	585	Baja California	1987	Cerro Prieto	Strike-Slip	C	5.5	3.95
10	825	Cape Mendocino	1992	Cape Mendocino	Reverse	C	7.01	3.5
11	3475	Chi-Chi, Taiwan-06	1999	TCU080	Reverse	C	6.3	5.1
12	879	Landers	1992	Lucerne	Strike-Slip	C	7.28	2.2
13	139	Tabas, Iran	1978	Dayhook	Reverse	C	7.35	6.95
14	727	Superstition Hills-02	1987	Superstition Mtn Camera	Strike-Slip	C	6.54	5.6
15	1611	Duzce, Turkey	1999	Lamont 1058	Strike-Slip	C	7.14	0.2
16	1618	Duzce, Turkey	1999	Lamont 53	Strike-Slip	C	7.14	8
17	106	Oroville-01	1975	Oroville Seismograph Station	Normal	C	5.89	7.9
18	156	Norcia, Italy	1979	Cascia	Normal	C	5.9	3.05
19	28	Parkfield	1966	Cholame - Shandon Array #12	Strike-Slip	C	6.19	17.6
20	71	San Fernando	1971	Lake Hughes #12	Reverse	C	6.61	16.65
21	125	Friuli- Italy-01	1976	Tolmezzo	Reverse	C	6.5	15.4

Table 4: Periods considered for "Range" based scaling method

Period #	1	2	3	4	5	6
Period (sec)	0.06	0.065	0.067	0.07	0.075	0.08
Period #	7	8	9	10	11	12
Period (sec)	0.085	0.09	0.095	0.1	0.11	0.12
Period #	13	14	15	16	17	18
Period (sec)	0.13	0.133	0.14	0.15	0.16	0.17
Period #	19	20	21	22	23	24
Period (sec)	0.18	0.19	0.2	0.22	0.24	0.25
Period #	25	26	27	28	29	30
Period (sec)	0.26	0.28	0.29	0.3	0.32	0.34
Period #	31	32	33	34	35	36
Period (sec)	0.35	0.36	0.38	0.4	0.42	0.44
Period #	37	38	39	40	41	42
Period (sec)	0.45	0.46	0.48	0.5	0.55	0.6

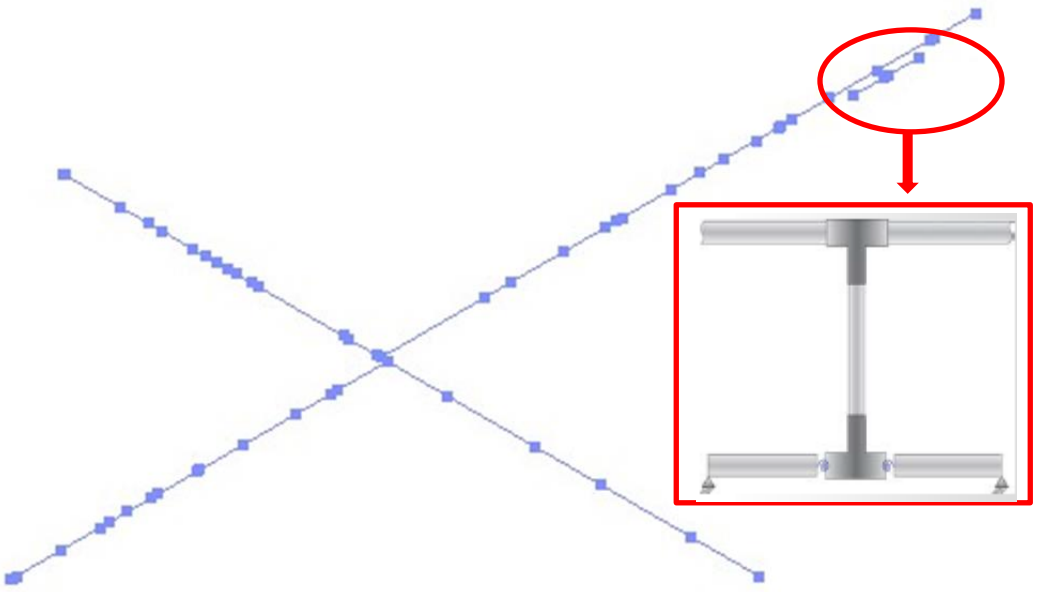

Figure 1: Piping System Configuration with Threaded Tee-joint at Single Location

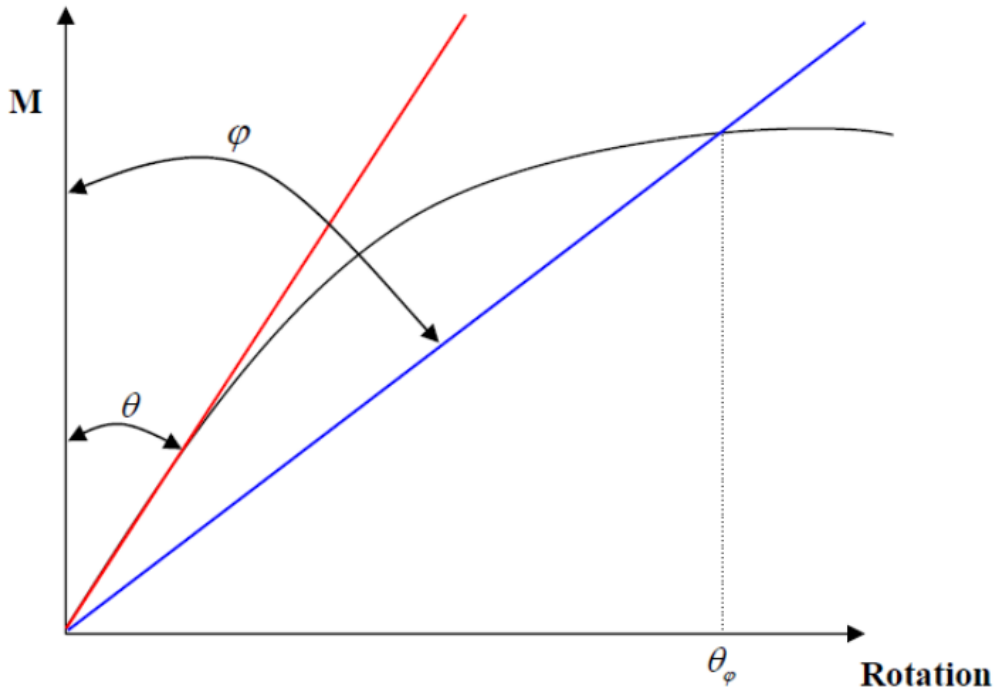

Figure 2: Characterization of Limit State (Ju, 2012)

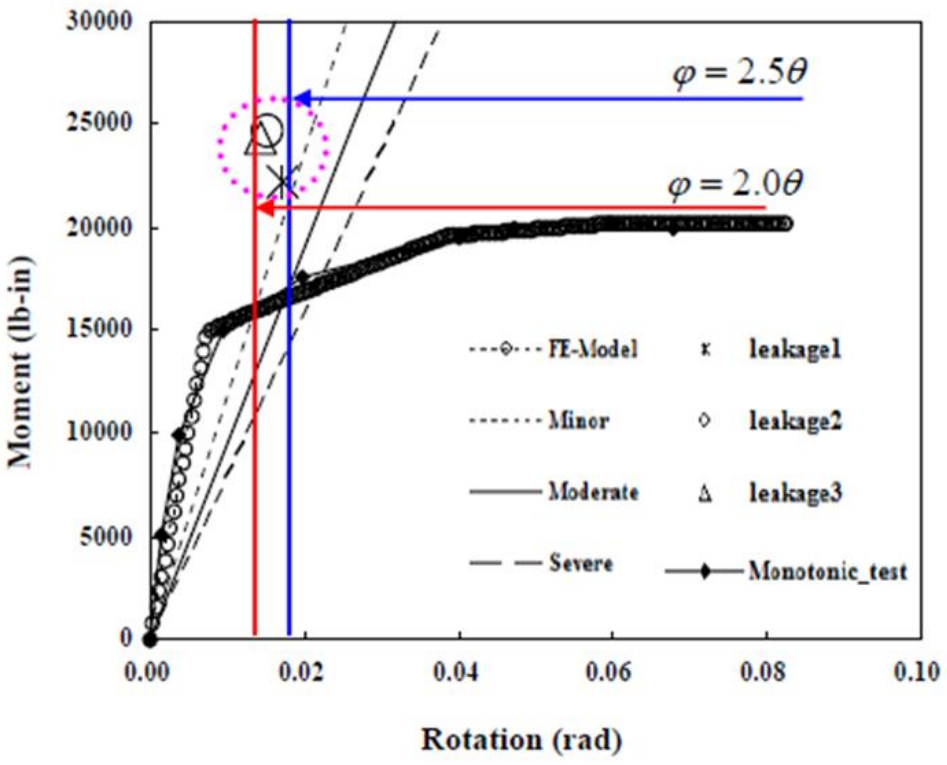

Figure 3: Rotations of 2-inch Black Iron Tee-joint for "First Leak" failure in Cyclic Tests (Ju, 2012)

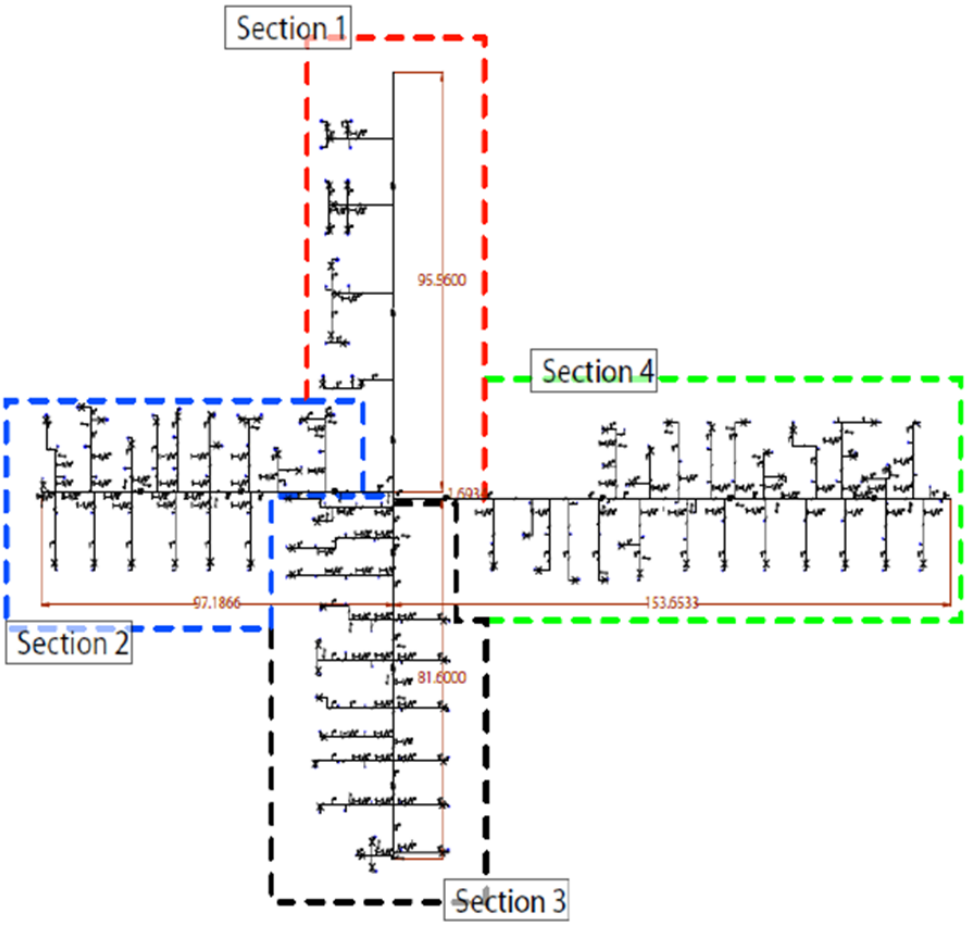

Figure 4: Hospital Piping System Layout (Ju, 2012)

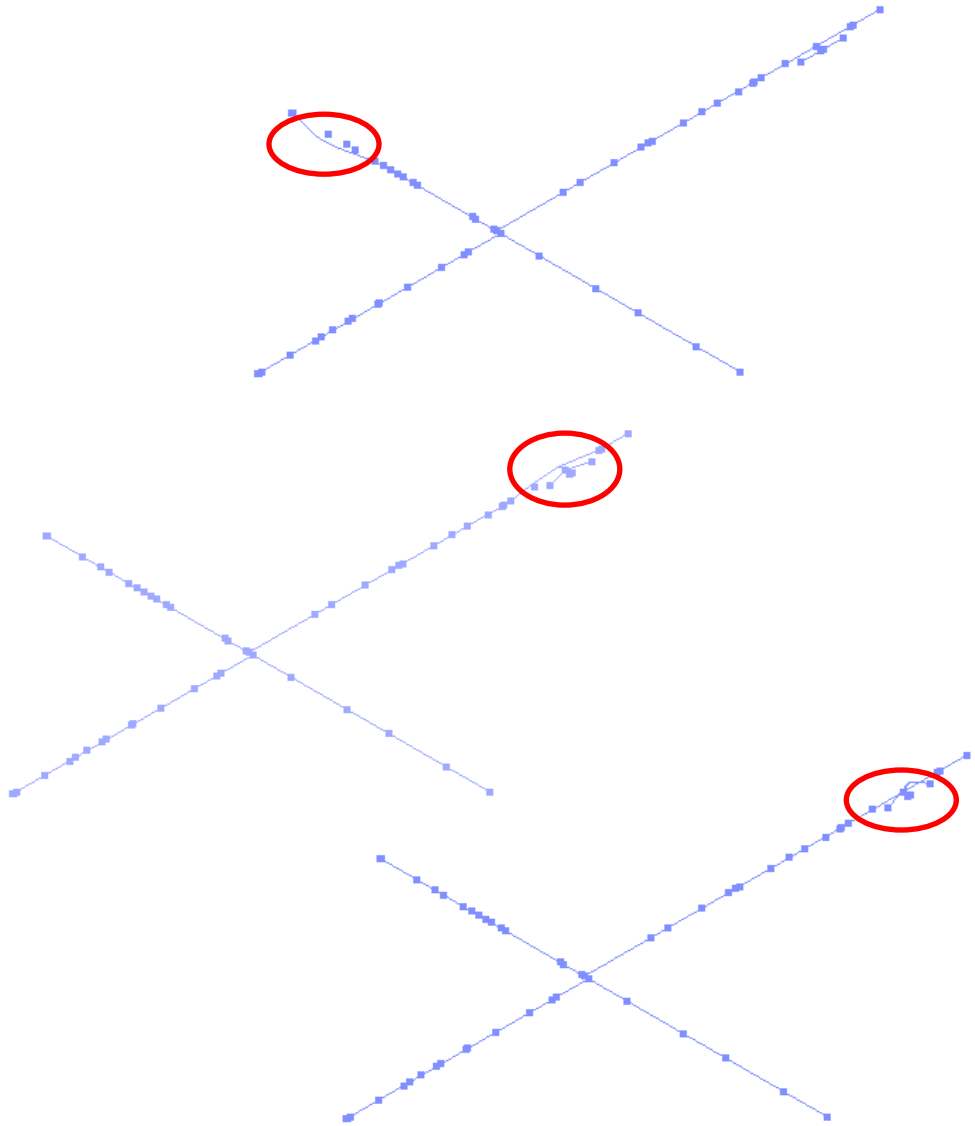

Figure 5: Global Fundamental Mode Shape (Upper Picture), Local Fundamental Mode Shape (Left Picture) and Local Second Mode Shape (Right Picture) Of the Piping System

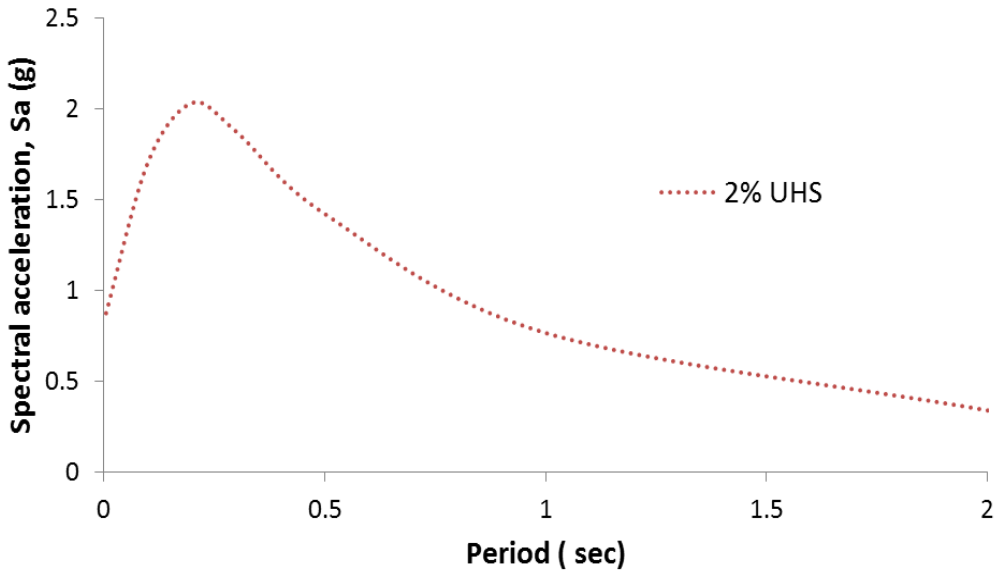

Figure 6: UHS with 2% of exceedance in 50 years at site of interest using USGS online hazard application (longitude 117.856 W, latitude 34.102, site class: C)

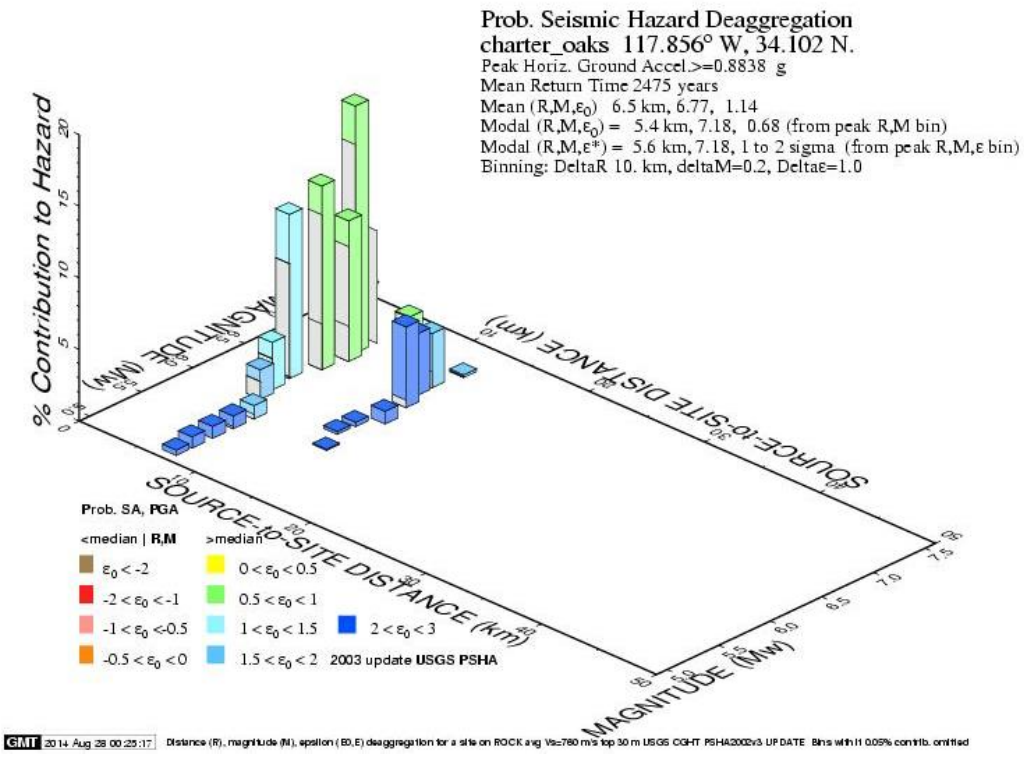

Figure 7: Probabilistic seismic hazard deaggregation at site of interest generated using 2002 version USGS interactive deaggregation tools (USGS, 2008b)

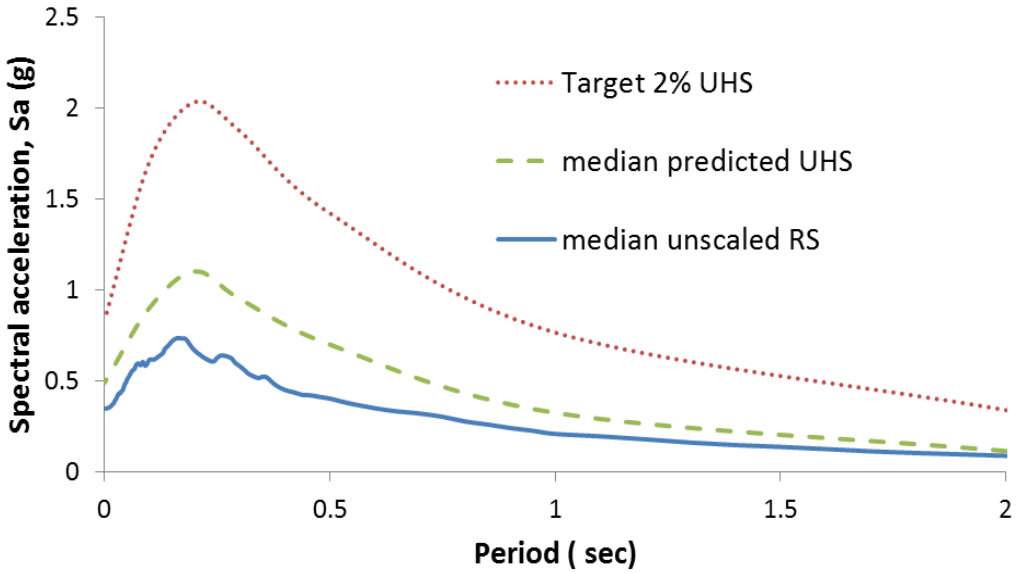

Figure 8: Median response spectrum (RS) of 21 unscaled ground motions versus 2% UHS and corresponding median predicted UHS

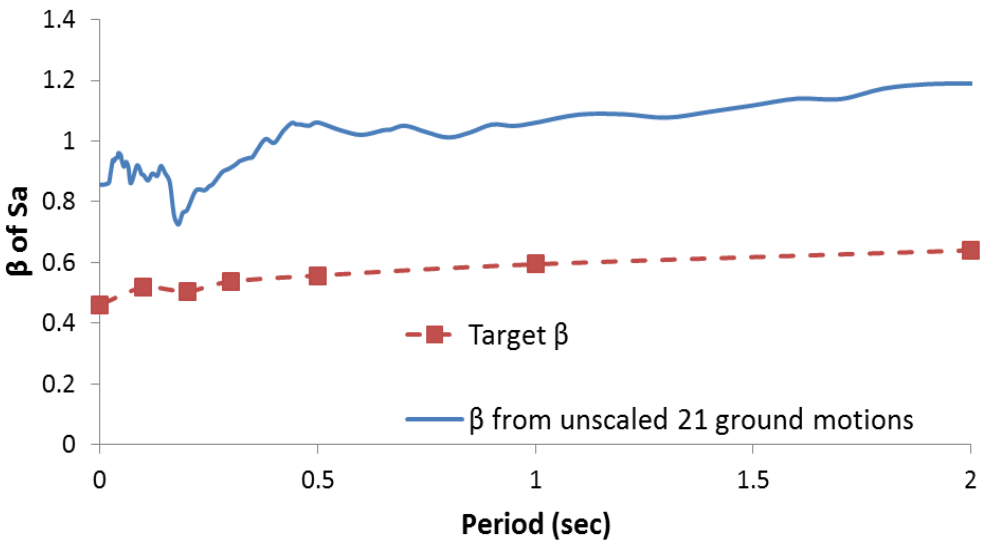

Figure 9: Logarithmic standard deviation (β) of 21 unscaled ground motions at the site of interest versus target β

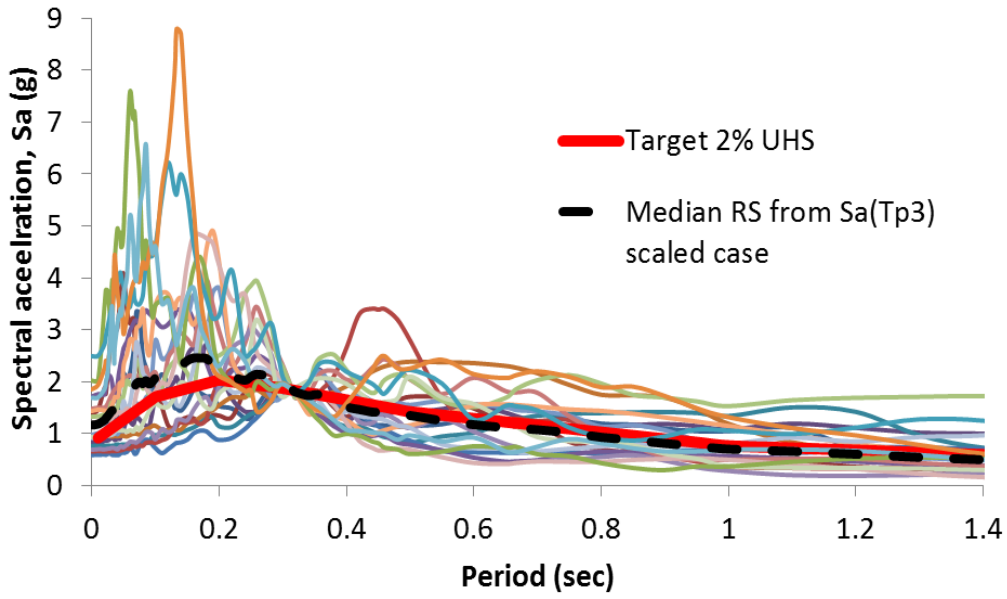

Figure 10a: Selected 21 ground motions scaled to match target 2% UHS at T_{p3}=0.315s

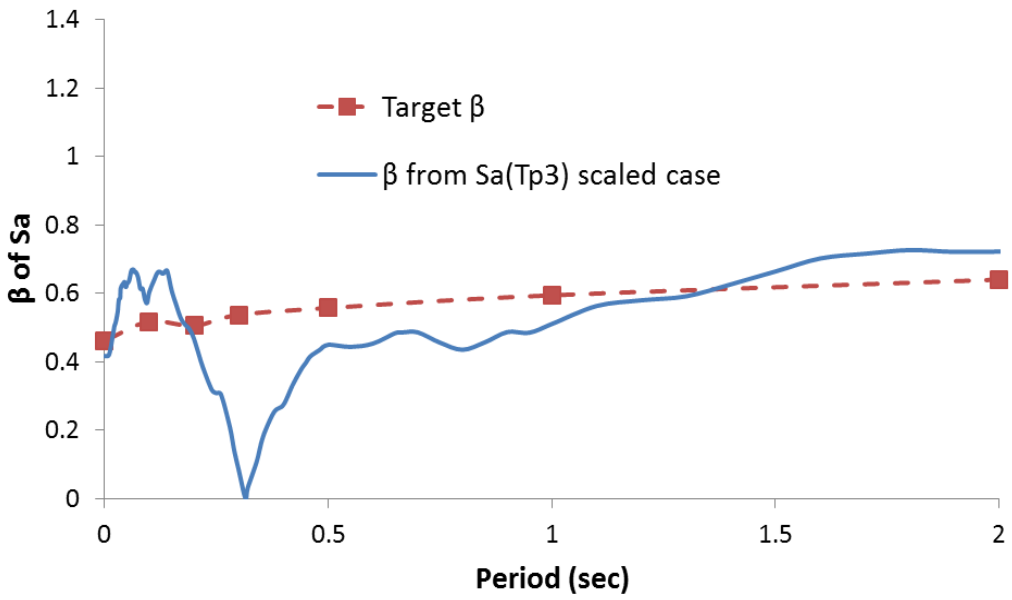

Figure 10b: Logarithmic standard deviation (β) of Sa(T_{p3}=0.315s) scaled 21 ground motions at the site of interest versus target β

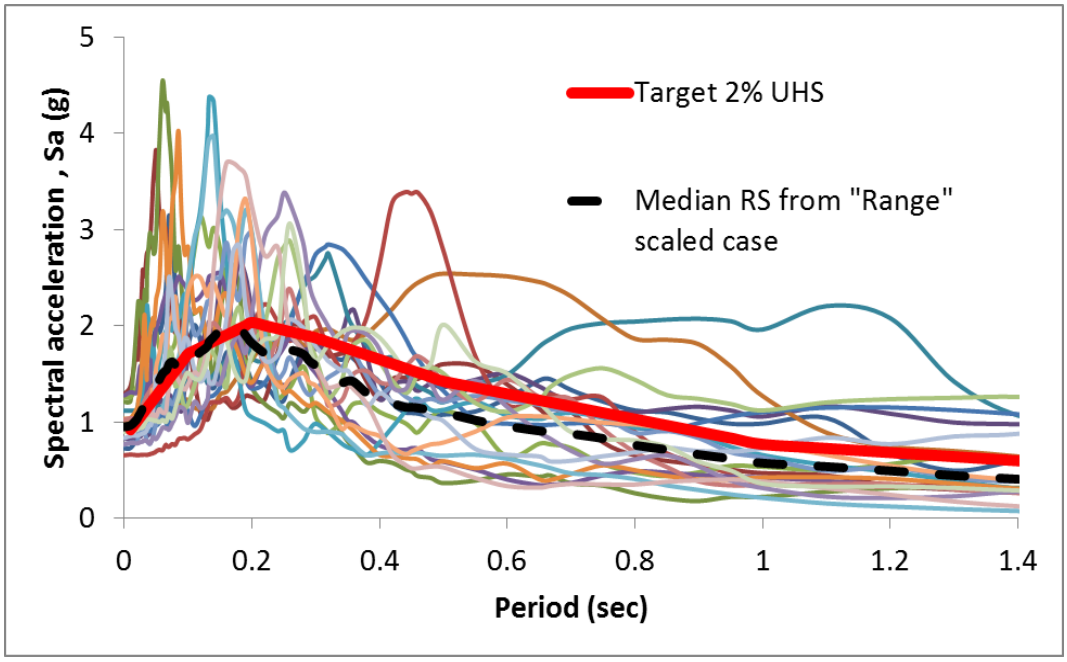

Figure 11a: Selected 21 ground motions scaled to match target 2% UHS over specified period range

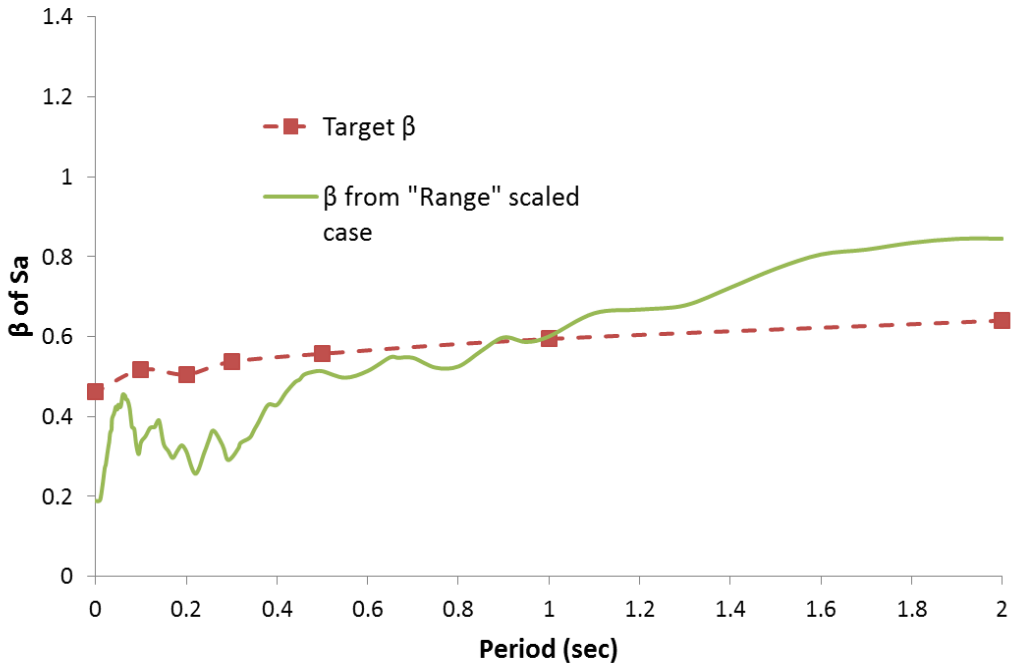

Figure 11b: Logarithmic standard deviation (β) of "Range" scaled 21 ground motions at the site of interest versus target β

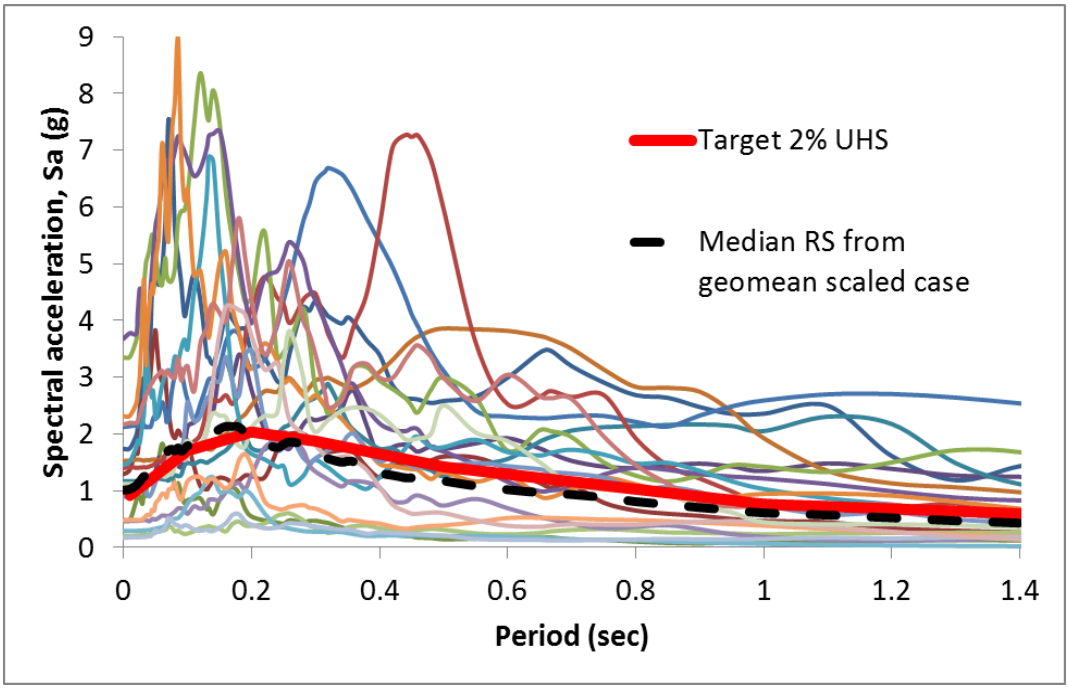

Figure 12a: Selected 21 ground motions scaled to match target 2% UHS by geomean scaling method

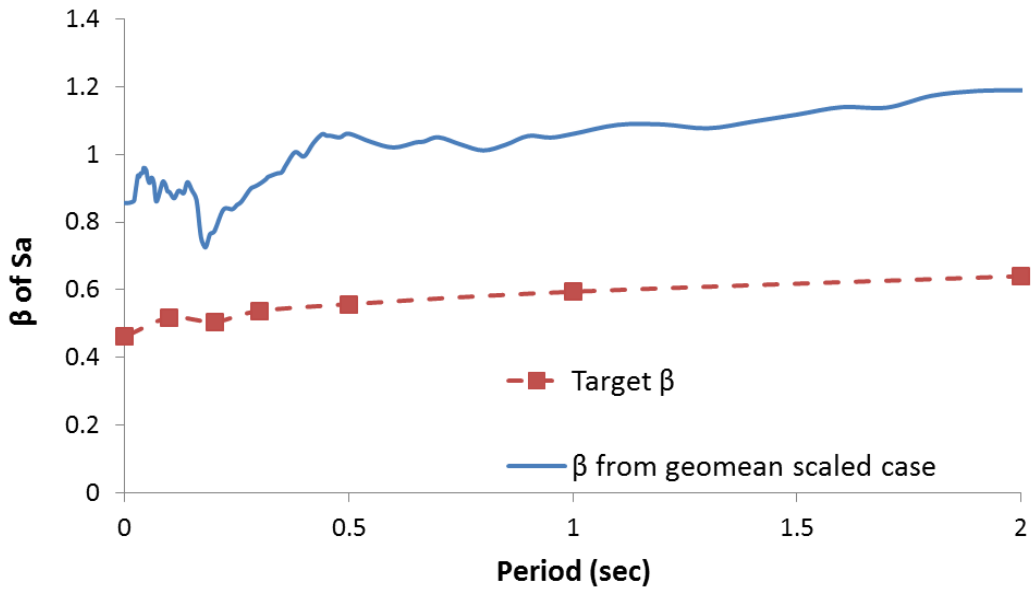

Figure 12b: Logarithmic standard deviation (β) of geometric mean scaled 21 ground motions at the site of interest versus target β

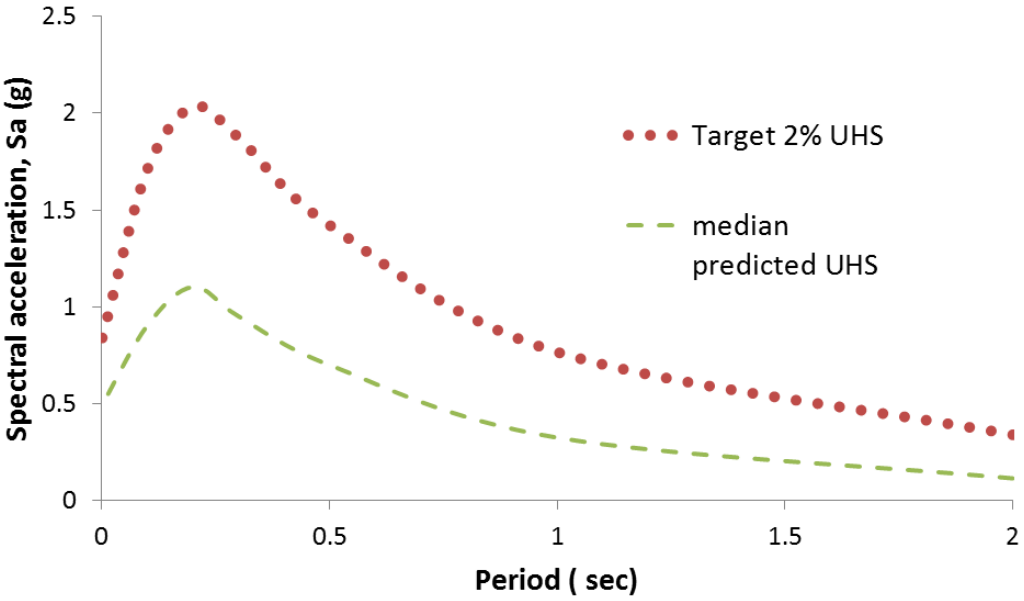

Figure 13: “Median” predicted UHS versus 2% UHS

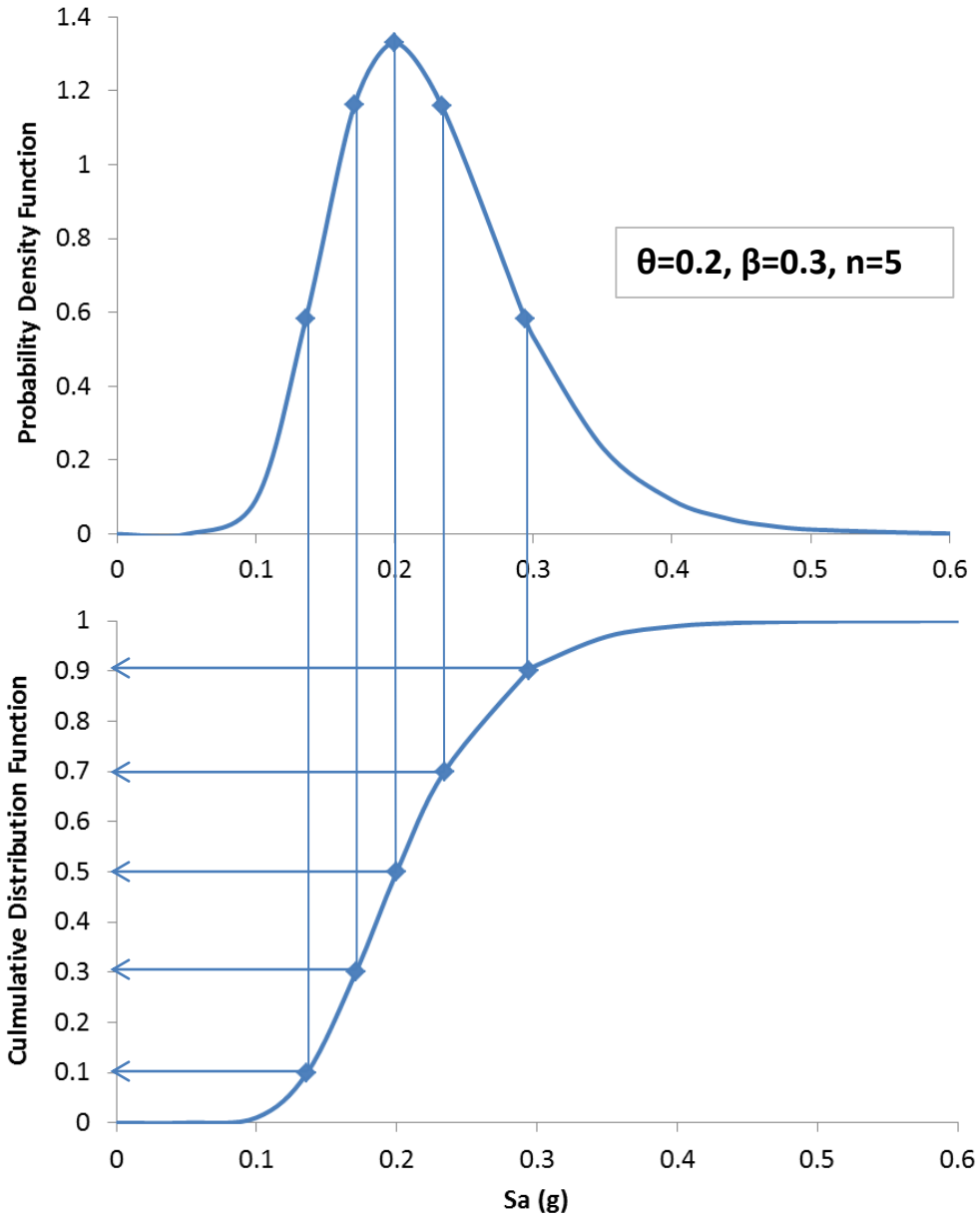

Figure 14: Example PDF and CDF for target spectral ordinates determination using D-Scaling method

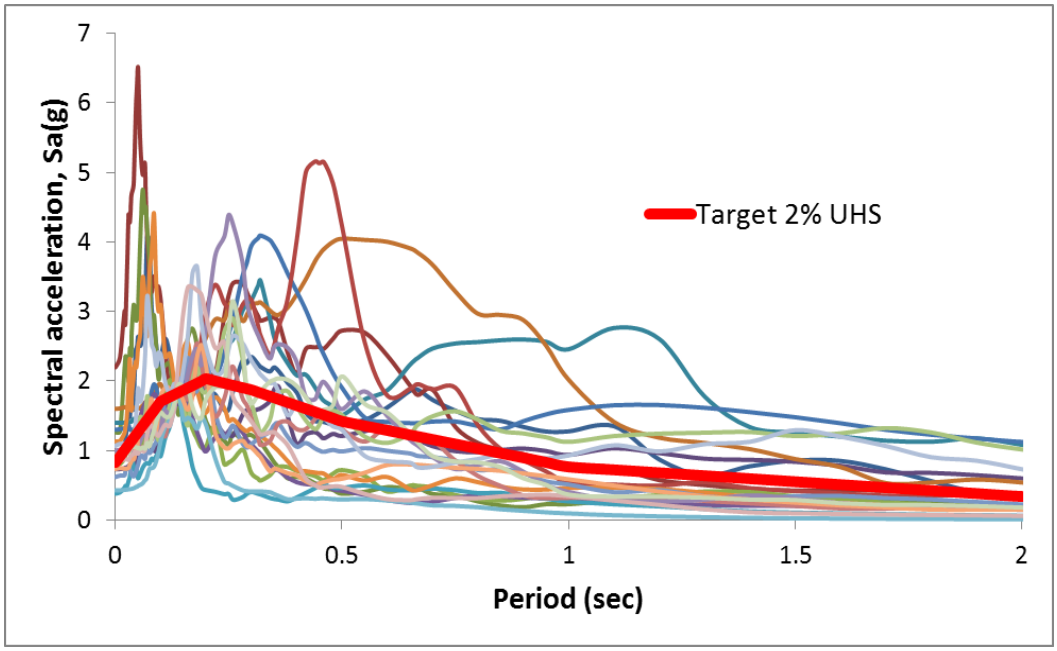

Figure 15a: Selected 21 ground motions scaled to match target 2% UHS at T_{p9}=0.136s

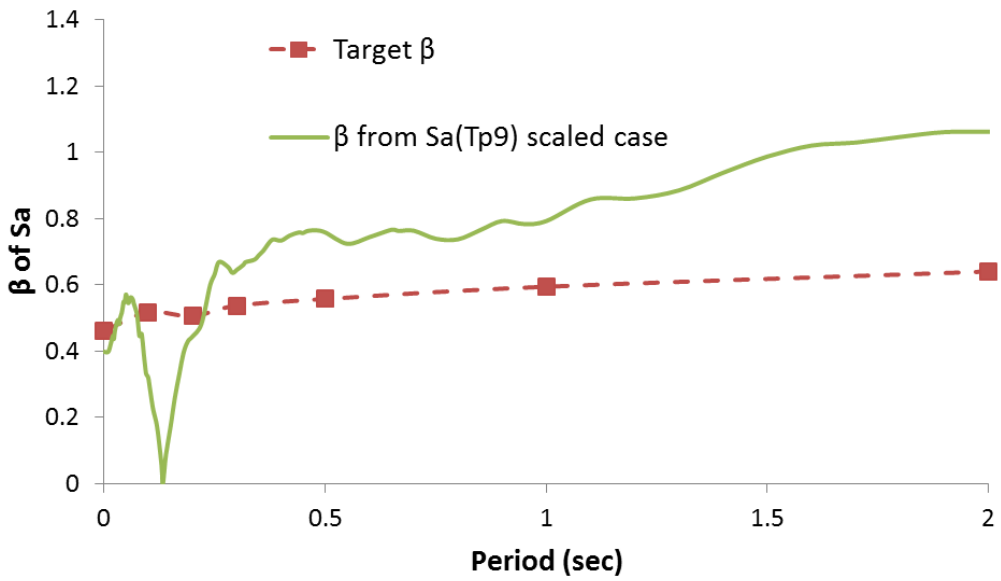

Figure 15b: Logarithmic standard deviation (β) of Sa(T_{p9}=0.136s) scaled 21 ground motions at the site of interest versus target β

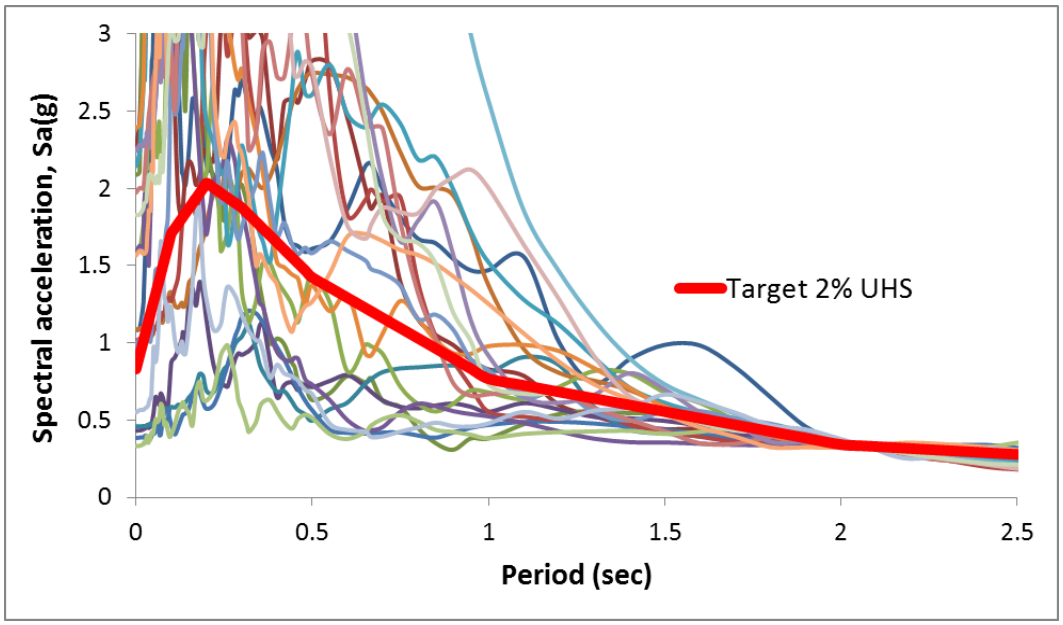

Figure 16a: Selected 21 ground motions scaled to match target 2% UHS at T_{b1}=2.07s (partial scale)

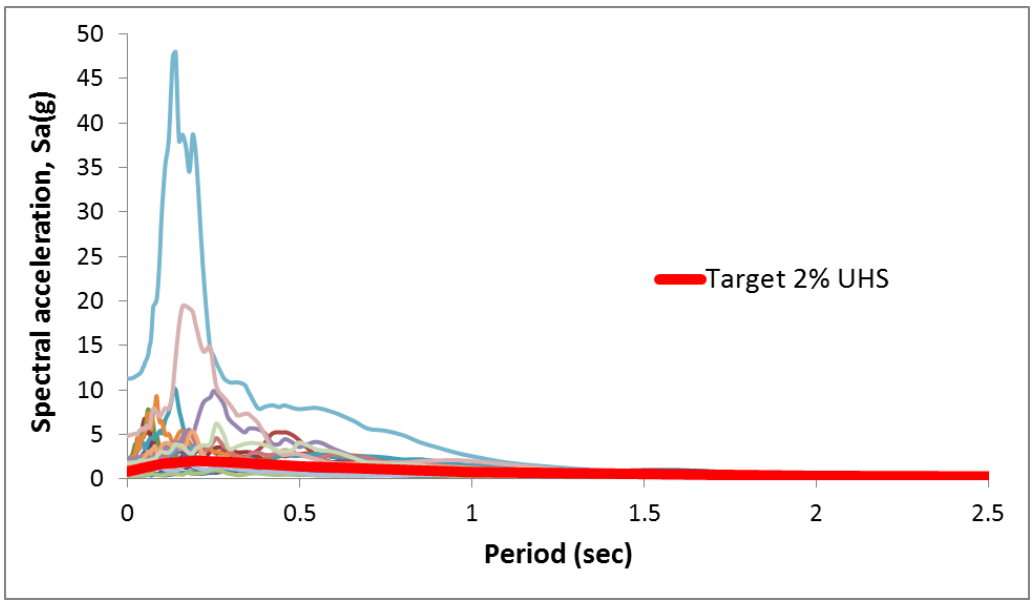

Figure 16b: Selected 21 ground motions scaled to match target 2% UHS at T_{b1}=2.07s (full scale)

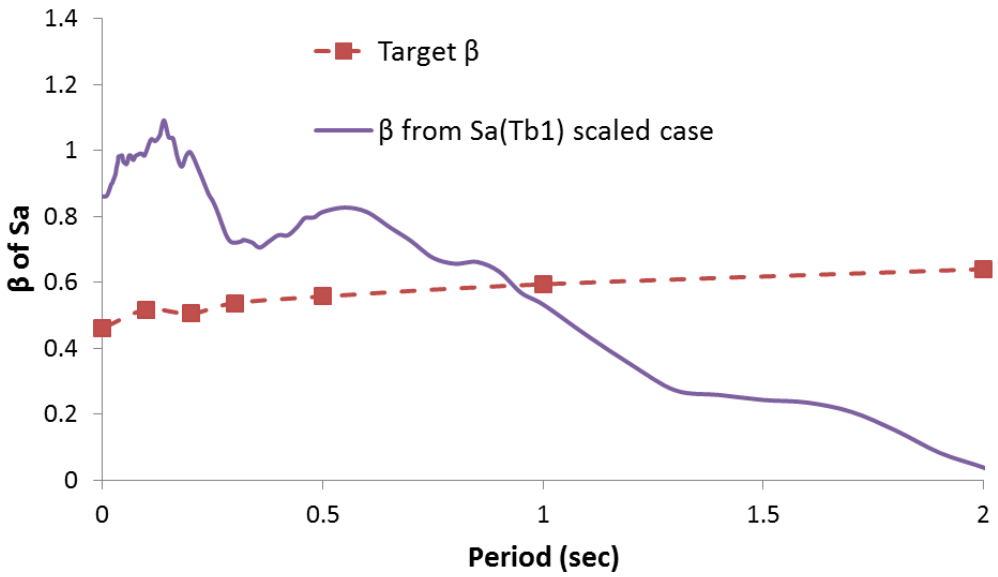

Figure 16c: Logarithmic standard deviation (β) of Sa(T_{b1}=2.07s) scaled 21 ground motions at the site of interest versus target β

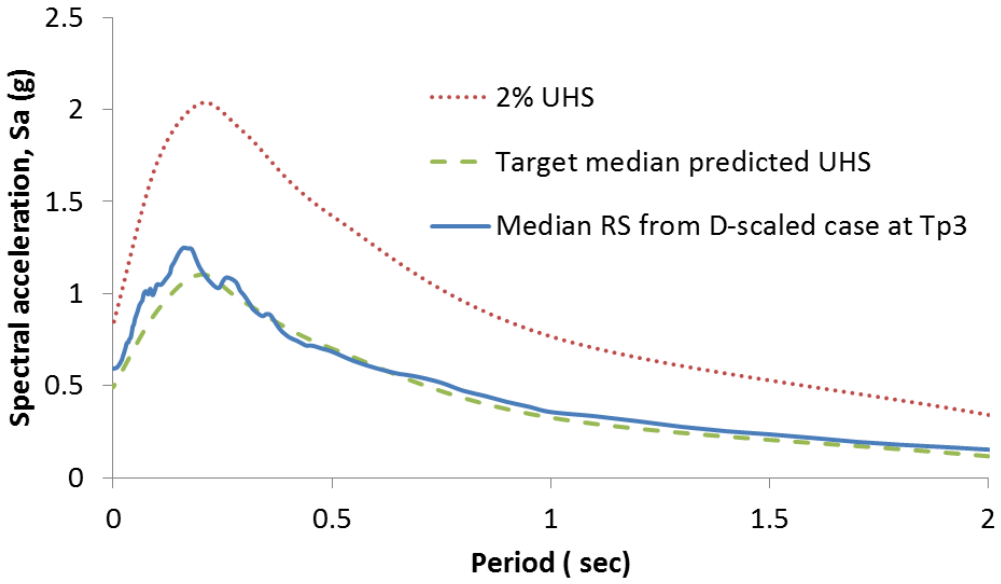

Figure 17a: Selected 21 ground motions scaled to match median predicted UHS at T_{p3}=0.315s

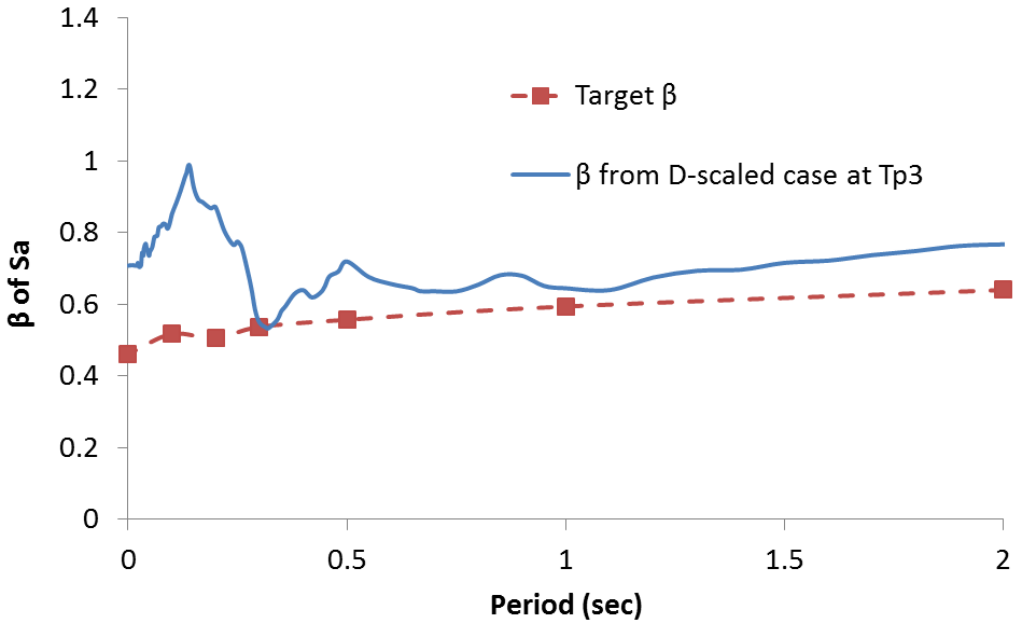

Figure 17b: Logarithmic standard deviation (β) of D-scaled 21 ground motions at the site of interest versus target β (targets at T_{p3}=0.315s)

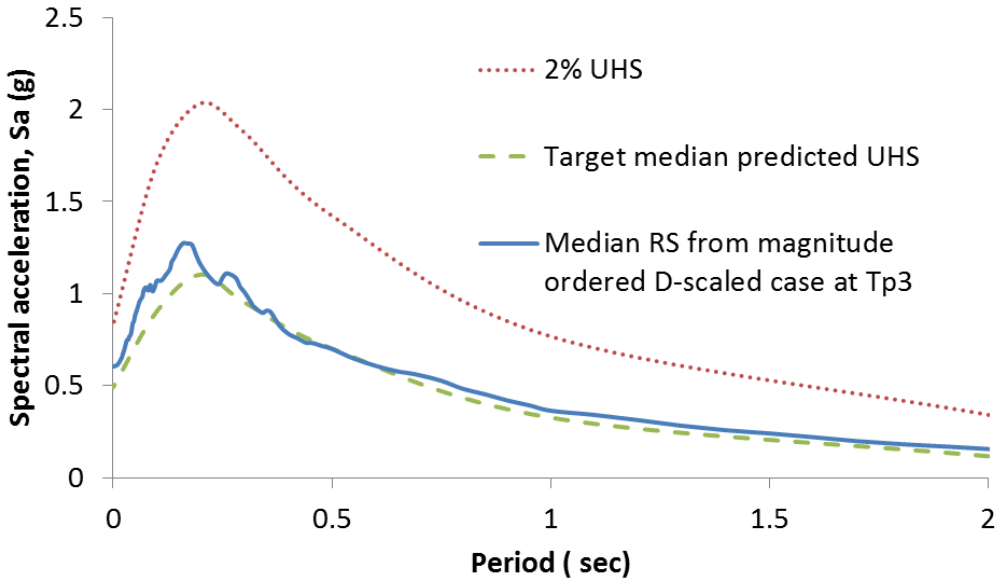

Figure 18a: Selected 21 ground motions scaled to match median predicted UHS at T_{p3}=0.315s

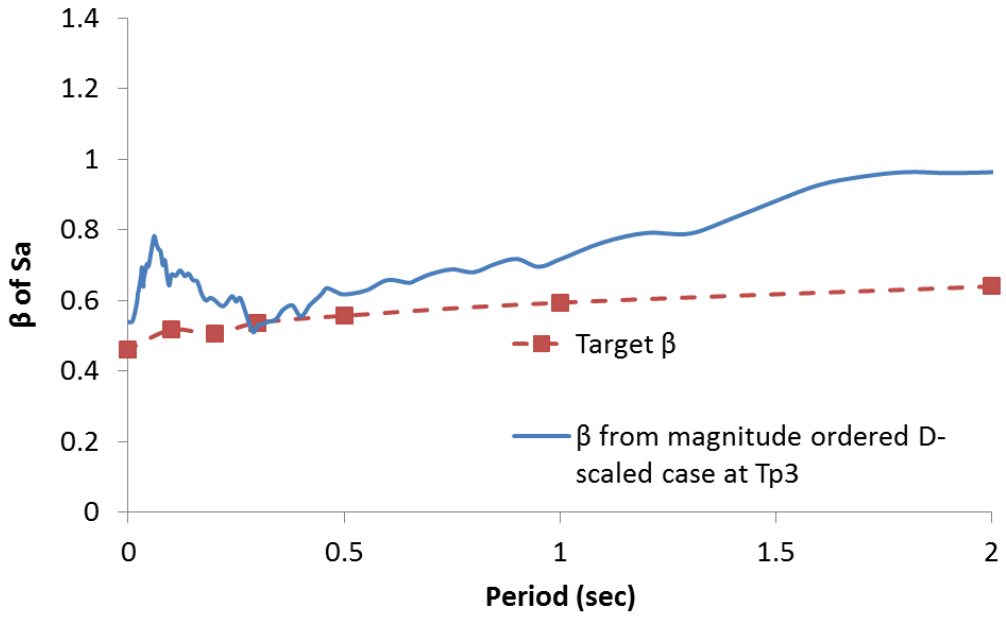

Figure 18b: Logarithmic standard deviation (β) of Magnitude ordered D-scaled 21 ground motions at the site of interest versus target β (targets at T_{p3}=0.315s)

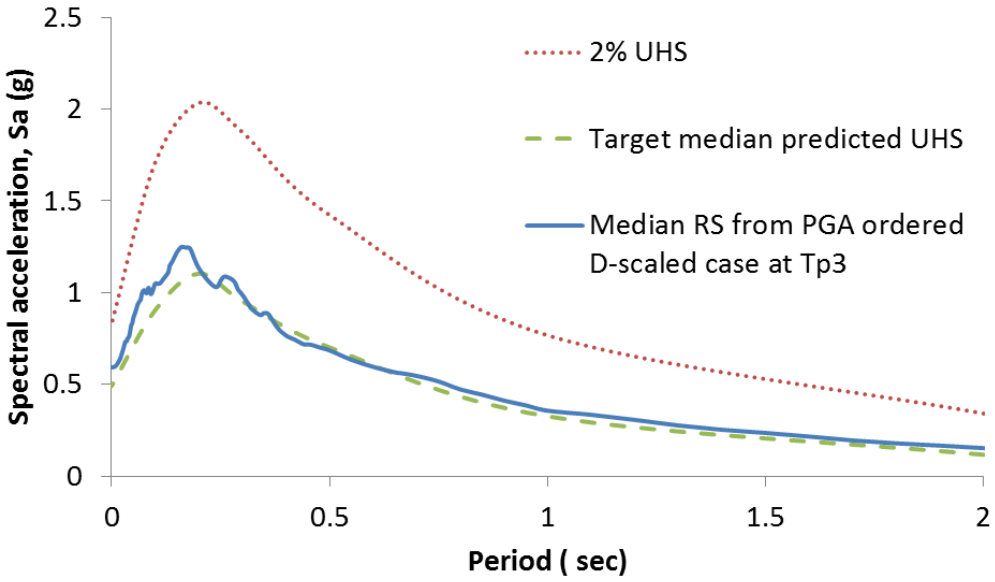

Figure 19a: Selected 21 ground motions scaled to match median predicted UHS at T_{p3}=0.315s

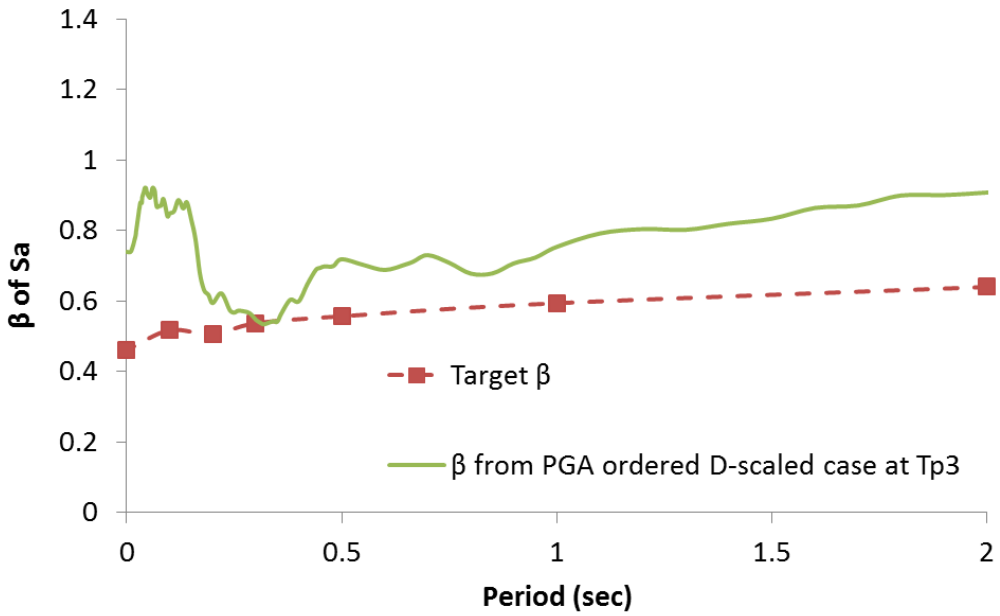

Figure 19b: Logarithmic standard deviation (β) of PGA ordered D-scaled 21 ground motions at the site of interest versus target β (targets at T_{p3}=0.315s)

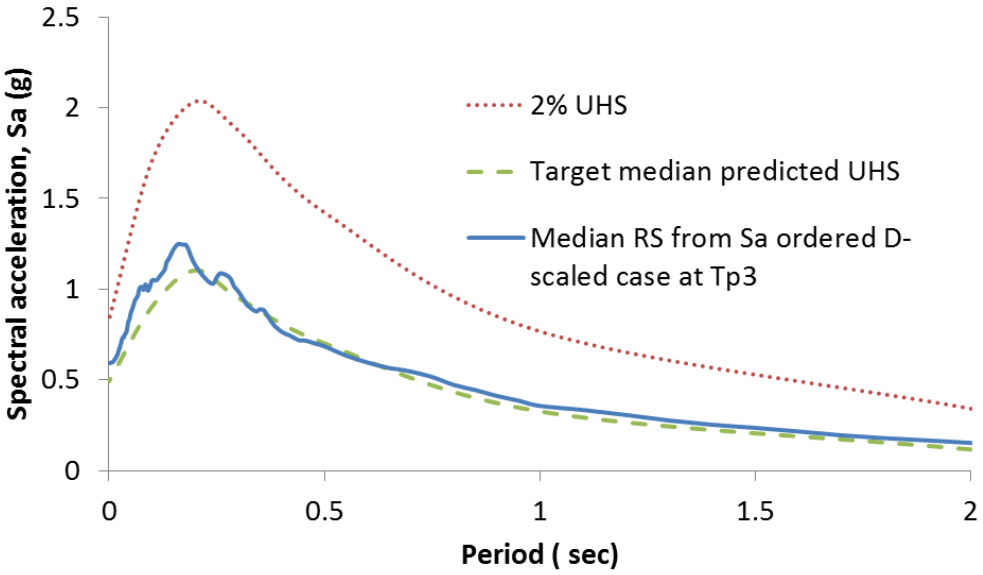

Figure 20a: Selected 21 ground motions scaled to match median predicted UHS at T_{p3}=0.315s

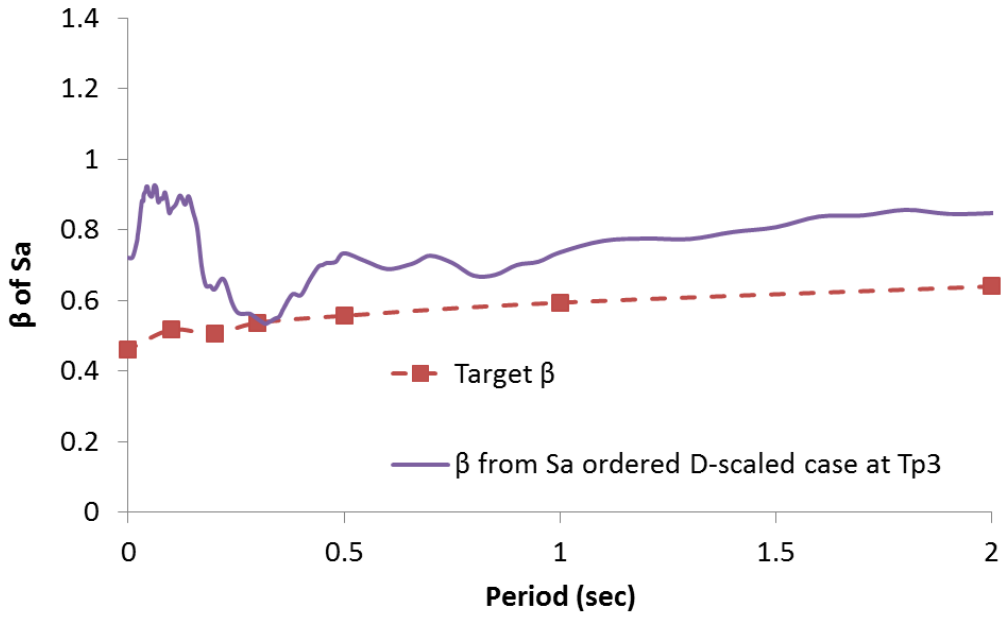

Figure 20b: Logarithmic standard deviation (β) of SA ordered D-scaled 21 ground motions at the site of interest versus target β (targets at T_{p3}=0.315s)

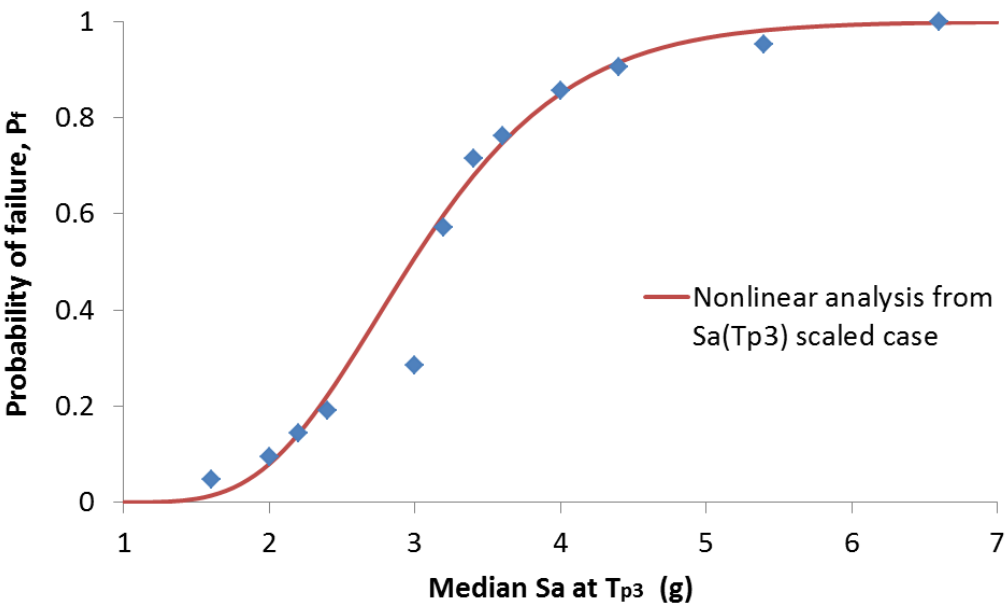

Figure 21: Nonlinear seismic fragility from Sa(T_{p3}) scaled ground motions

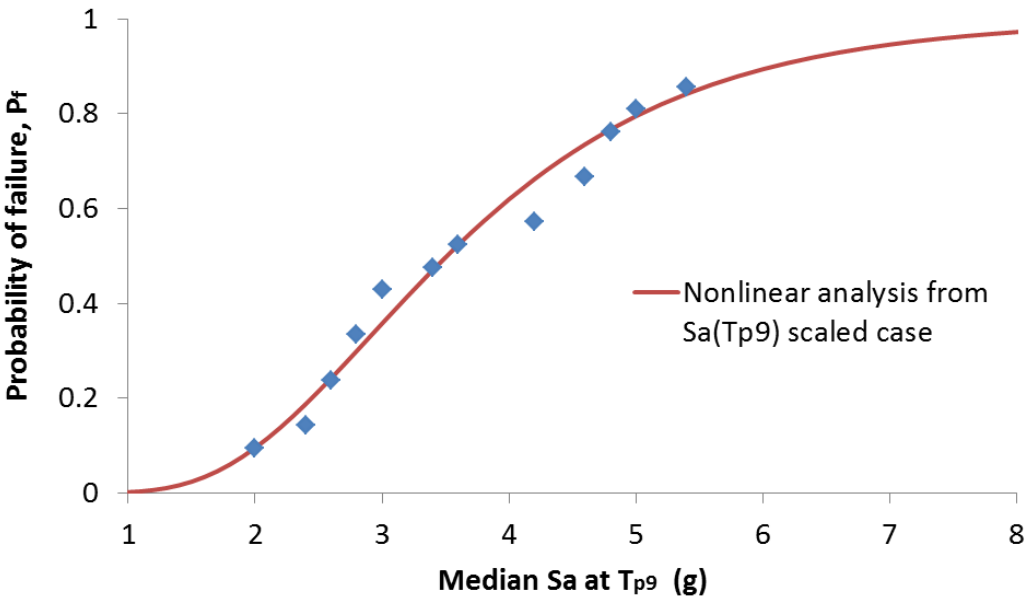

Figure 22: Nonlinear seismic fragility from Sa(T_{p9}) scaled ground motions

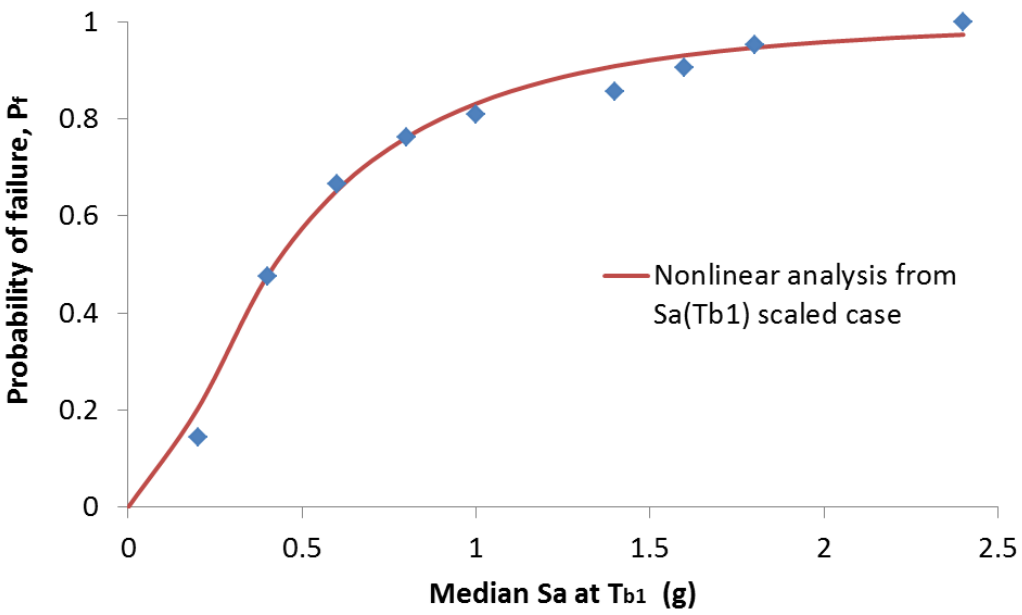

Figure 23: Nonlinear seismic fragility from Sa(T_{b1}) scaled ground motions

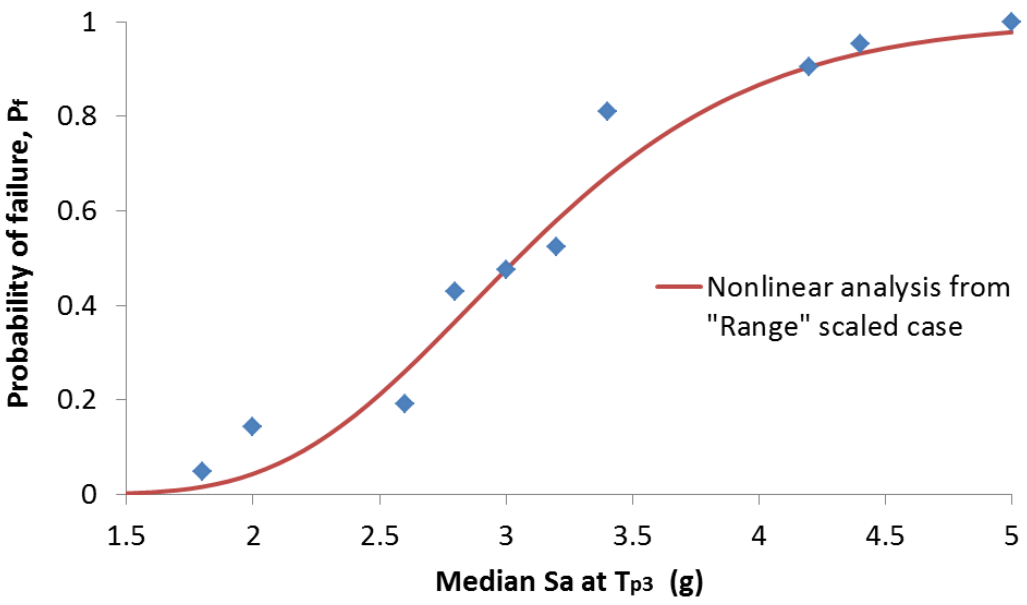

Figure 24: Nonlinear seismic fragility from “Range” scaled ground motions

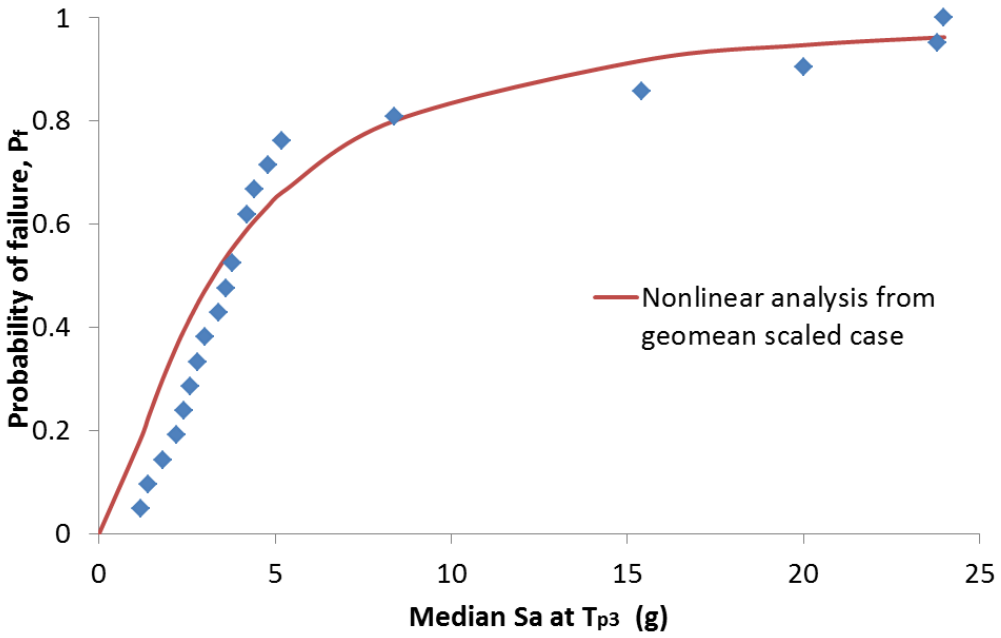

Figure 25: Nonlinear seismic fragility from geomean scaled ground motions

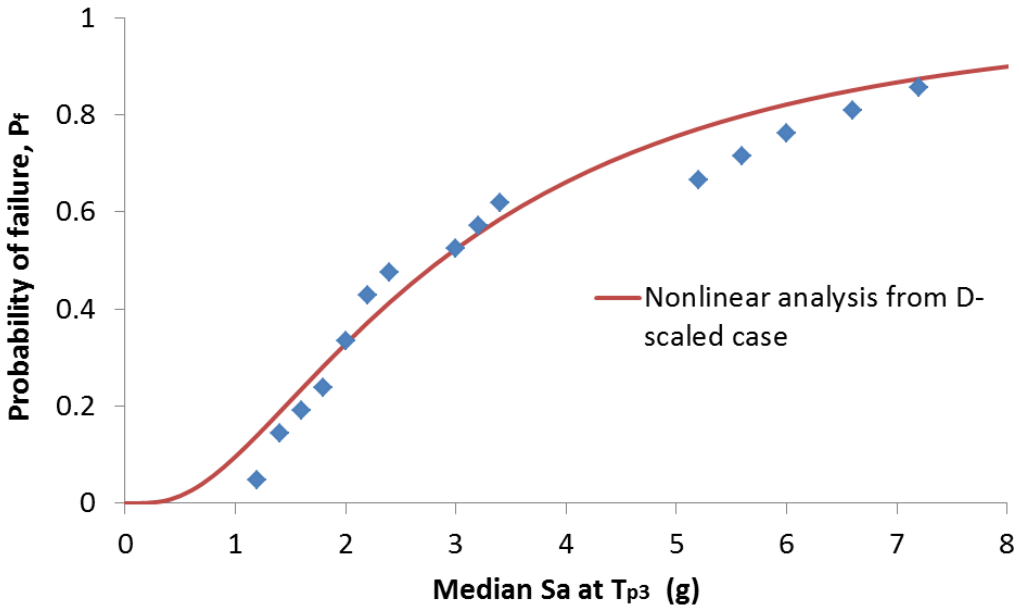

Figure 26: Nonlinear seismic fragility from D-scaled ground motions

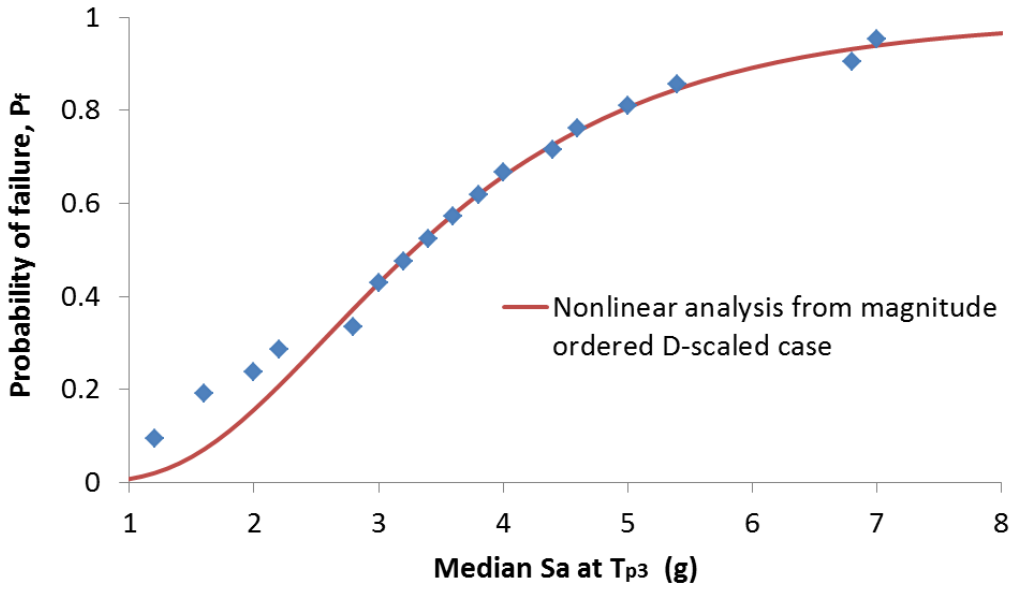

Figure 27: Nonlinear seismic fragility from Magnitude ordered D-scaled ground motions

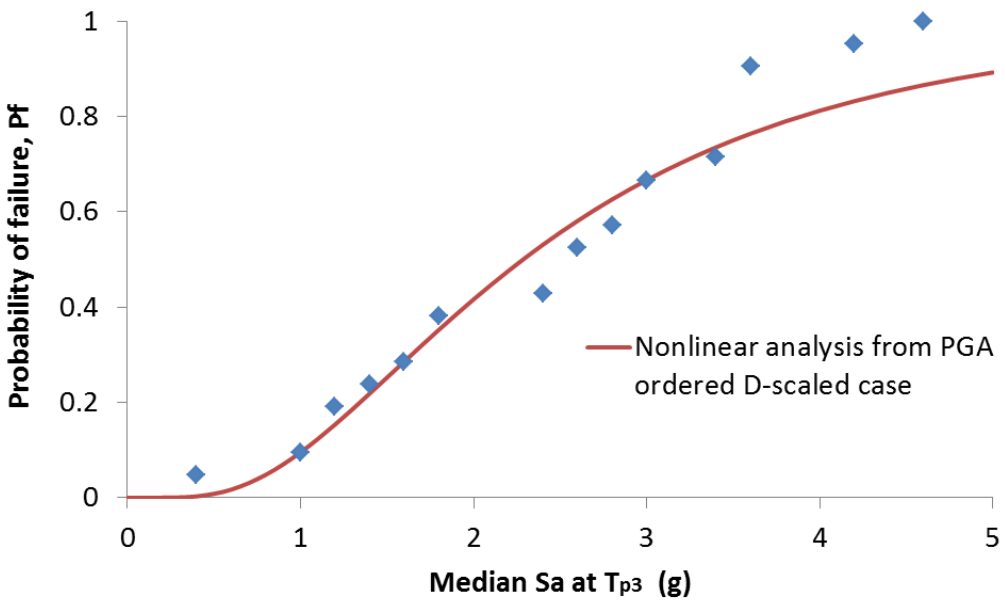

Figure 28: Nonlinear seismic fragility from PGA ordered D-scaled ground motions

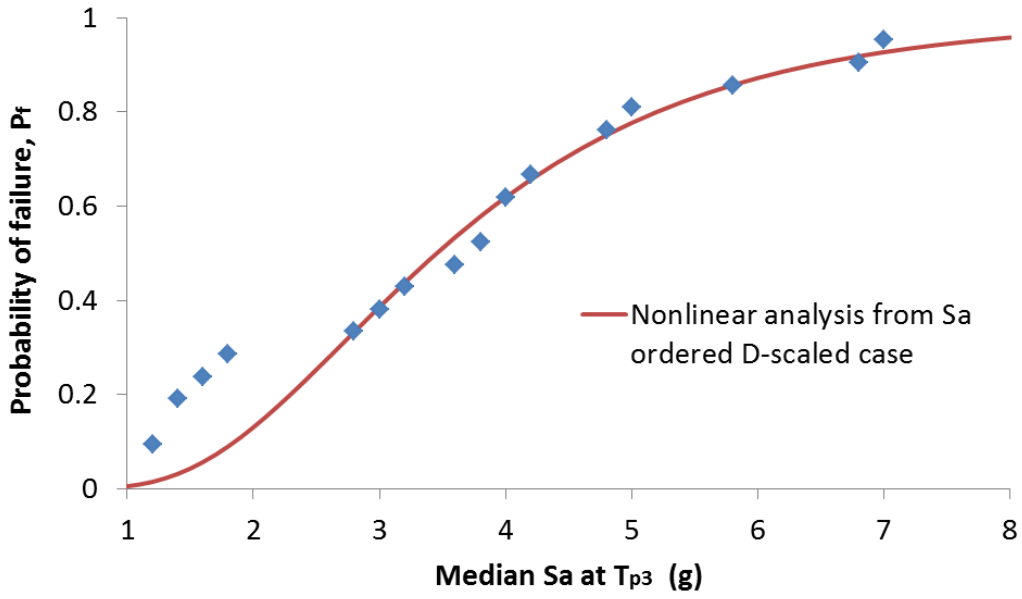

Figure 29: Nonlinear seismic fragility from SA ordered D-scaled ground motions

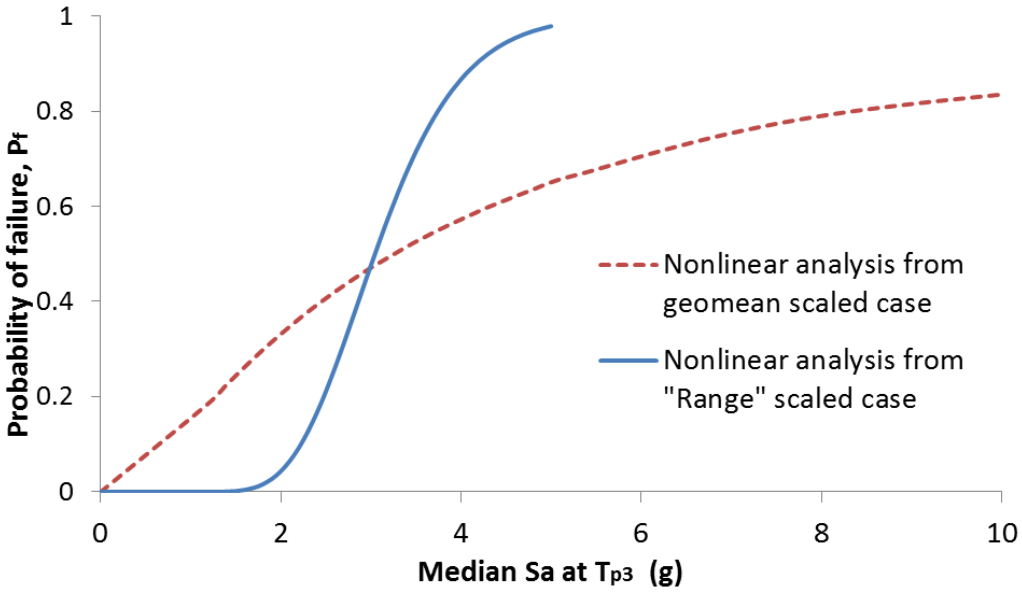

Figure 30: Seismic fragility from different scaling methods listed in this study (Part I)

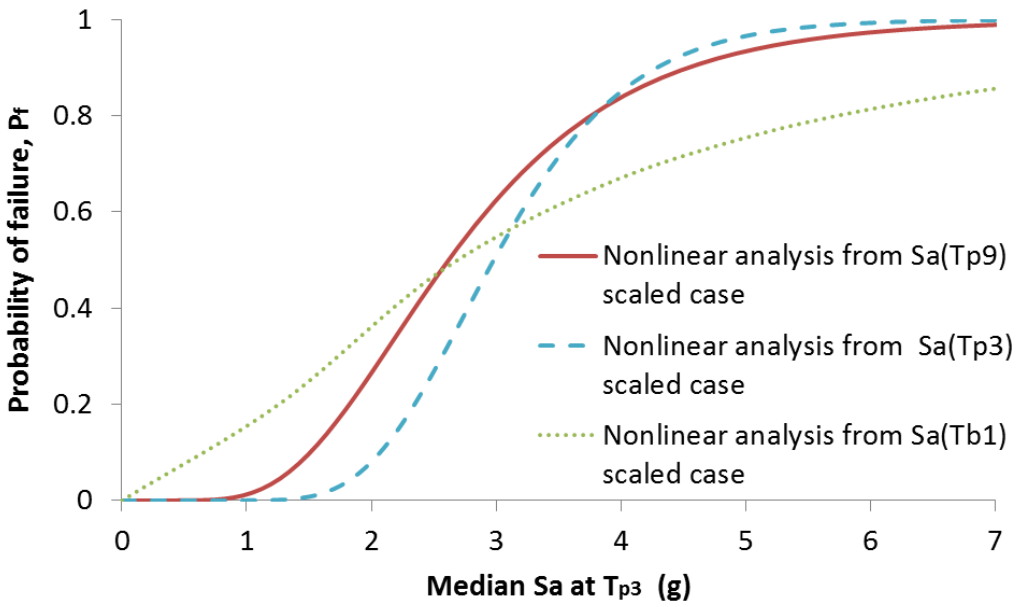

Figure 31: Seismic fragility from different scaling methods listed in this study (Part II)

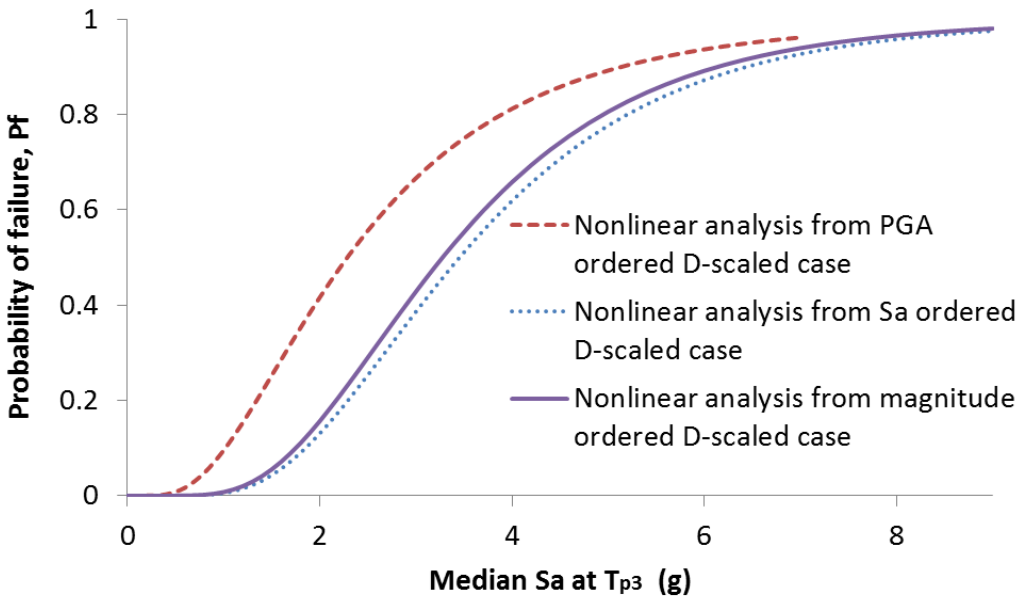

Figure 32: Seismic fragility from different scaling methods listed in this study (Part III)

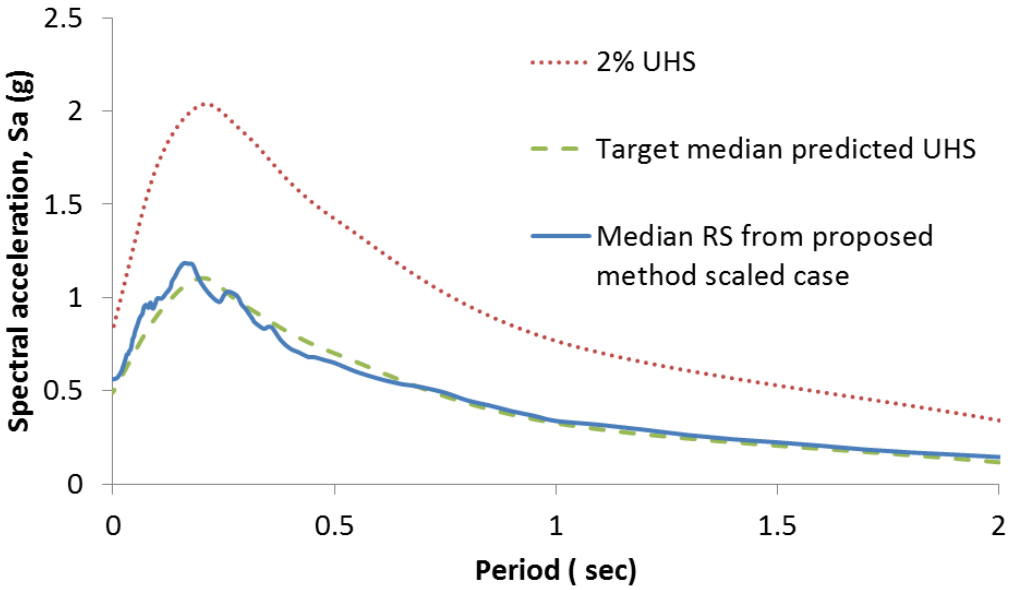

Figure 33a: Selected 21 ground motions scaled to match median predicted UHS

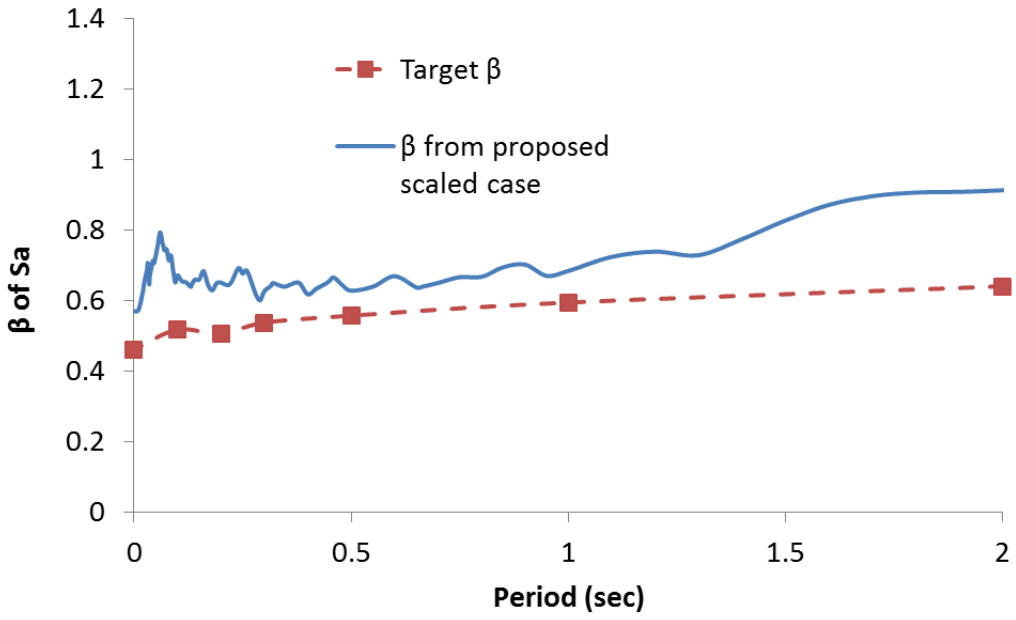

Figure 33b: Logarithmic standard deviation (β) of proposed scaled 21 ground motions at the site of interest versus target β

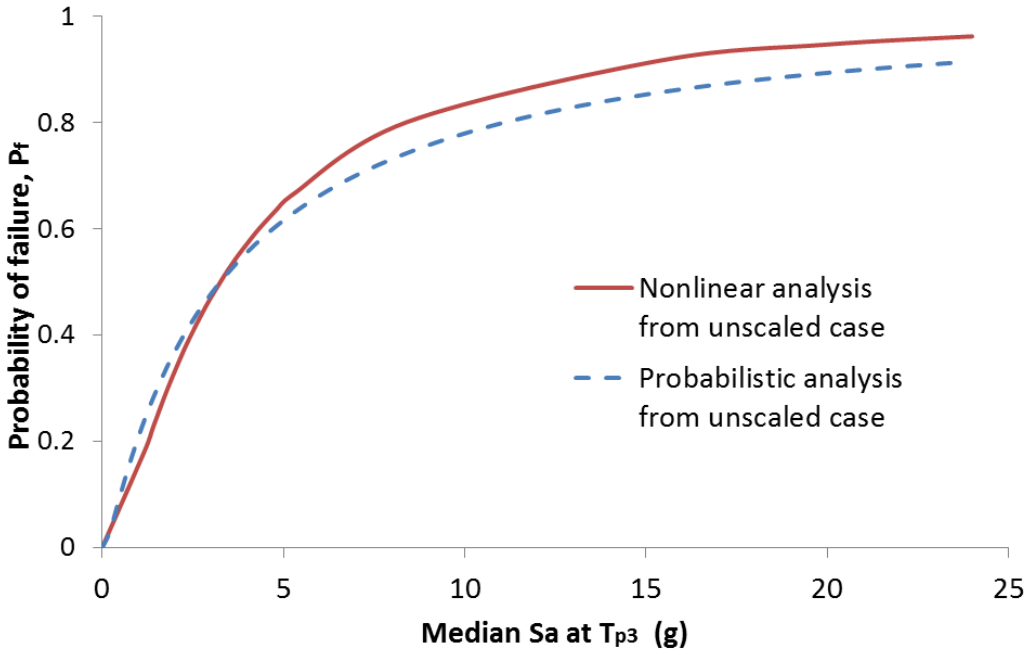

Figure 34: Seismic fragility of piping Tee-joint from unscaled ground motions: nonlinear FE analysis versus probabilistic analysis

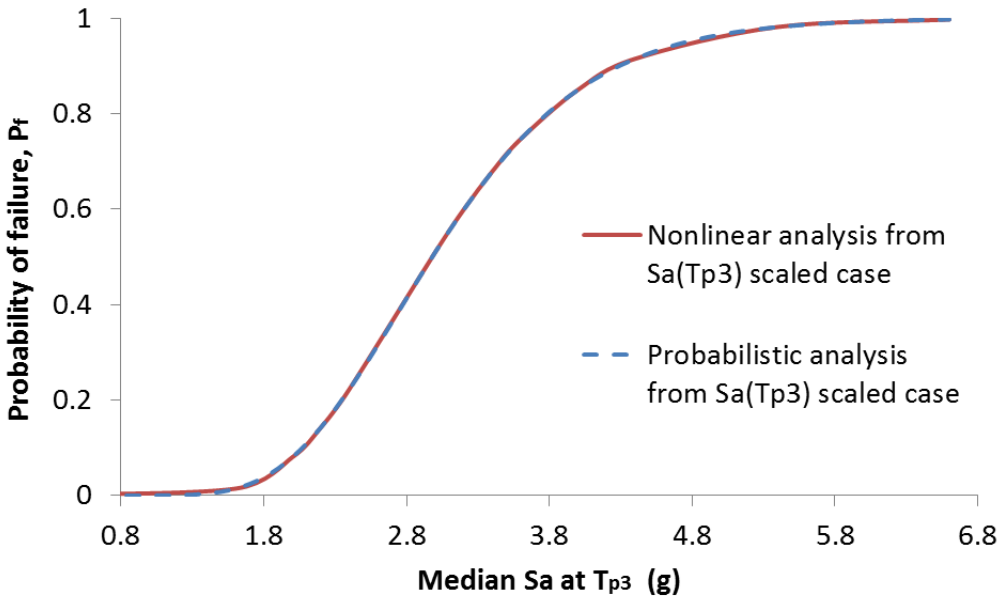

Figure 35: Seismic fragility of piping Tee-joint from single period (T_{p3}) scaled ground motions: nonlinear FE analysis versus probabilistic analysis

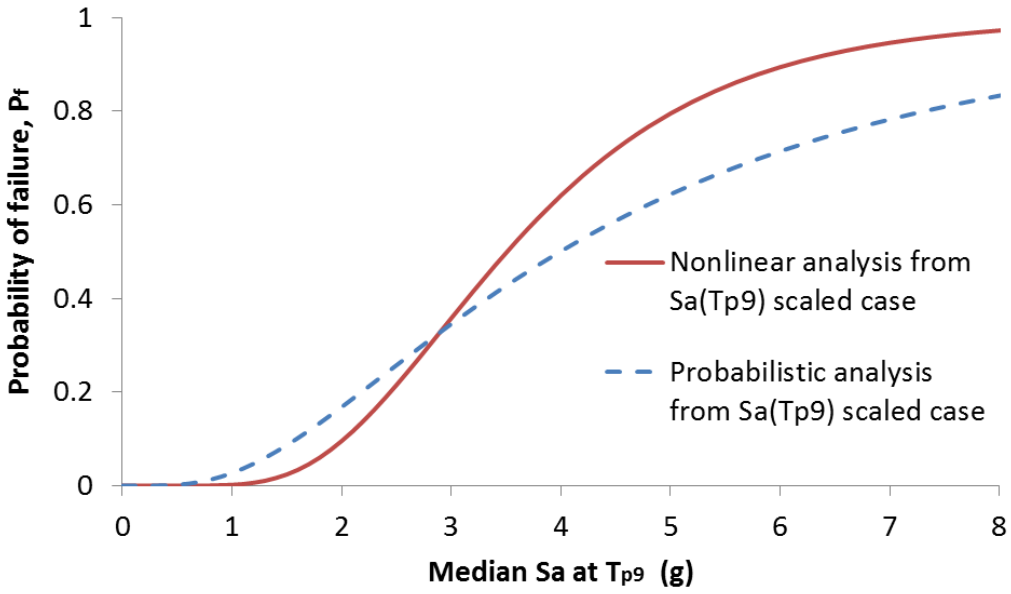

Figure 36: Seismic fragility of piping Tee-joint from single period (T_{p9}) scaled ground motions: nonlinear FE analysis versus probabilistic analysis

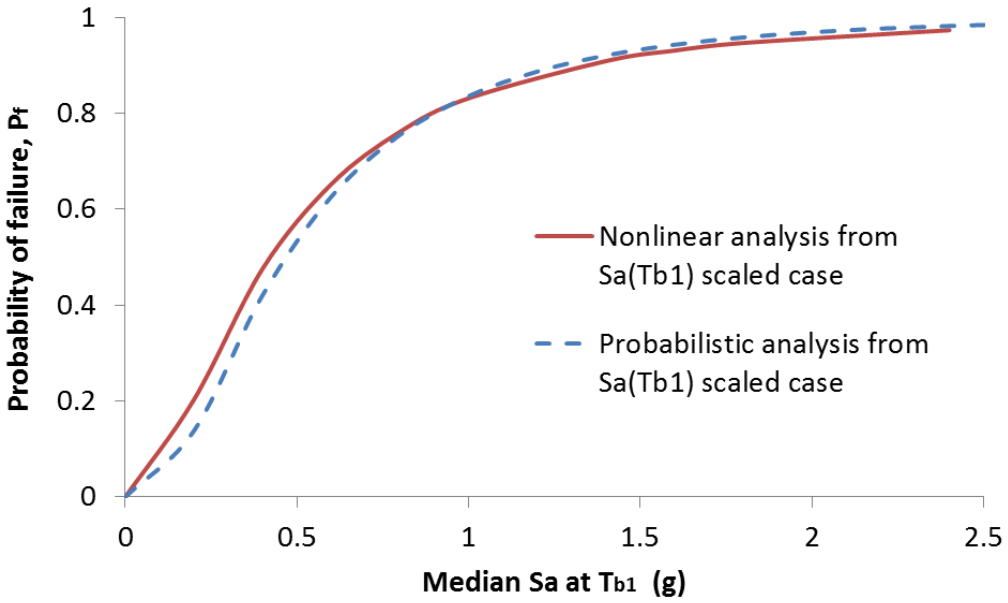

Figure 37: Seismic fragility of piping Tee-joint from single period (T_{b1}) scaled ground motions: nonlinear FE analysis versus probabilistic analysis

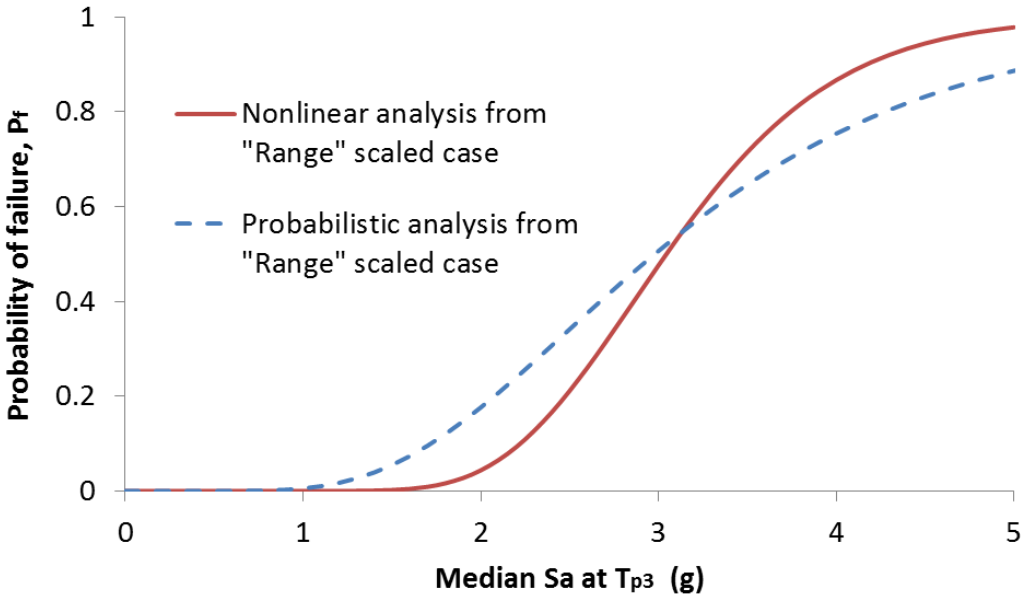

Figure 38: Seismic fragility of piping Tee-joint from “Range” based scaled ground motions: nonlinear FE analysis versus probabilistic analysis

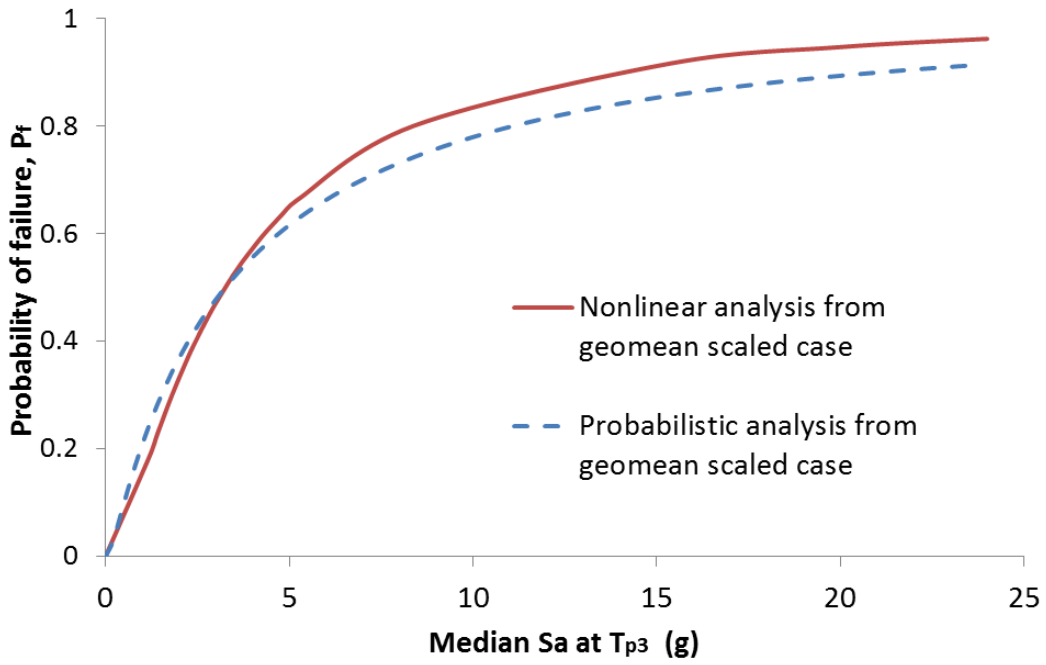

Figure 39: Seismic fragility of piping Tee-joint from geometric mean based scaled ground motions: nonlinear FE analysis versus probabilistic analysis (same as unscaled case)

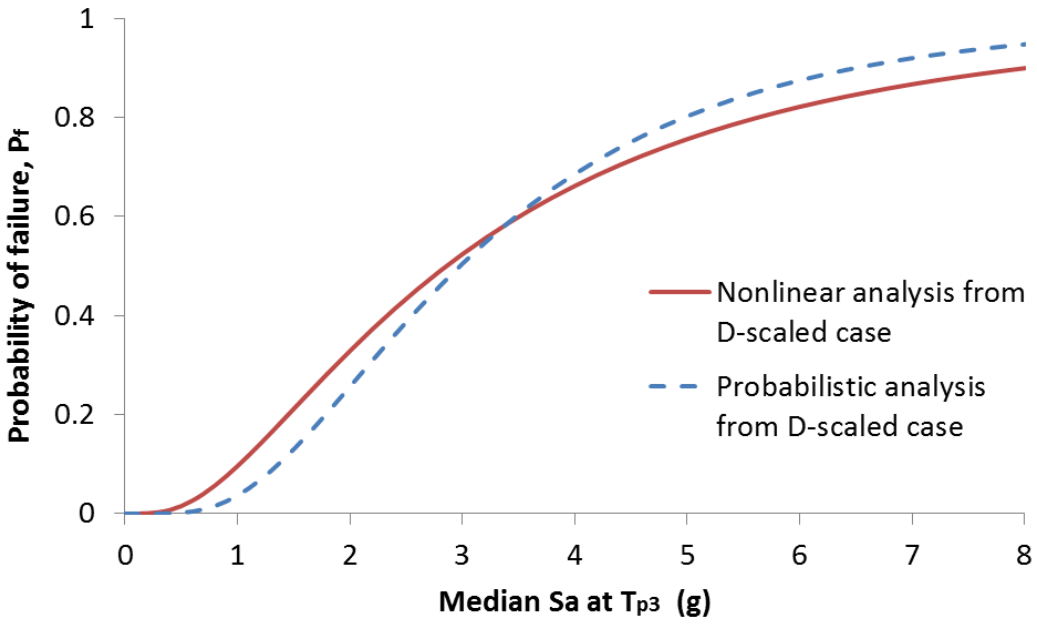

Figure 40: Seismic fragility of piping Tee-joint from D-scaled ground motions: nonlinear FE analysis versus probabilistic analysis

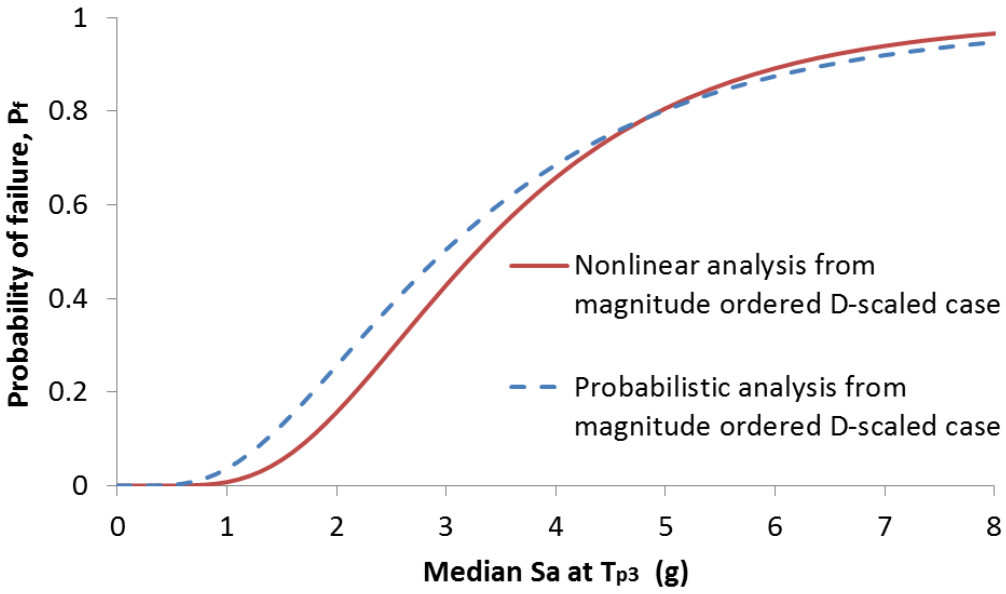

Figure 41: Seismic fragility of piping Tee-joint from Magnitude ordered D-scaled ground motions: nonlinear FE analysis versus probabilistic analysis

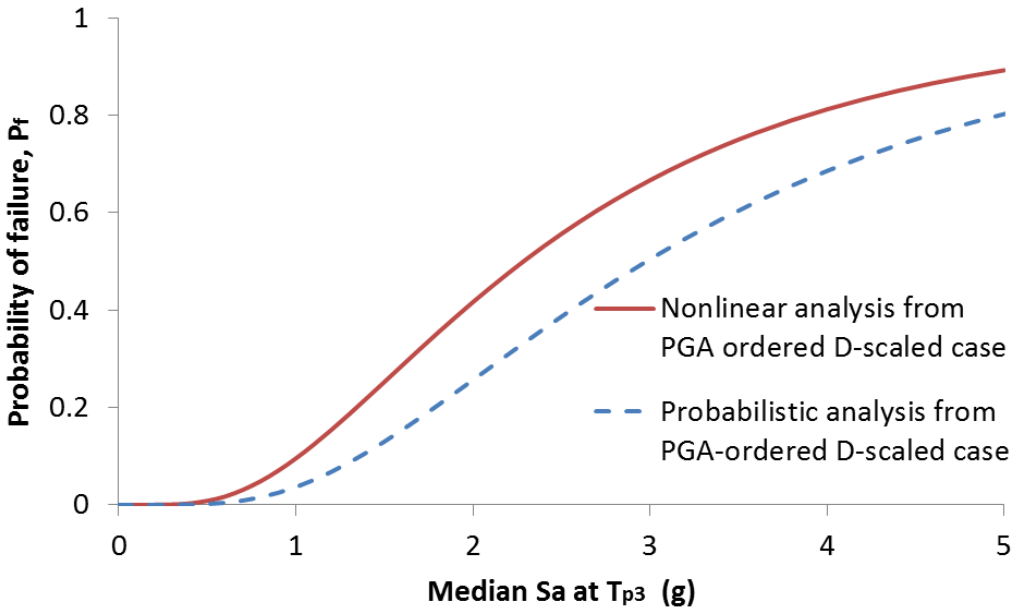

Figure 42: Seismic fragility of piping Tee-joint from PGA ordered D-scaled ground motions: nonlinear FE analysis versus probabilistic analysis

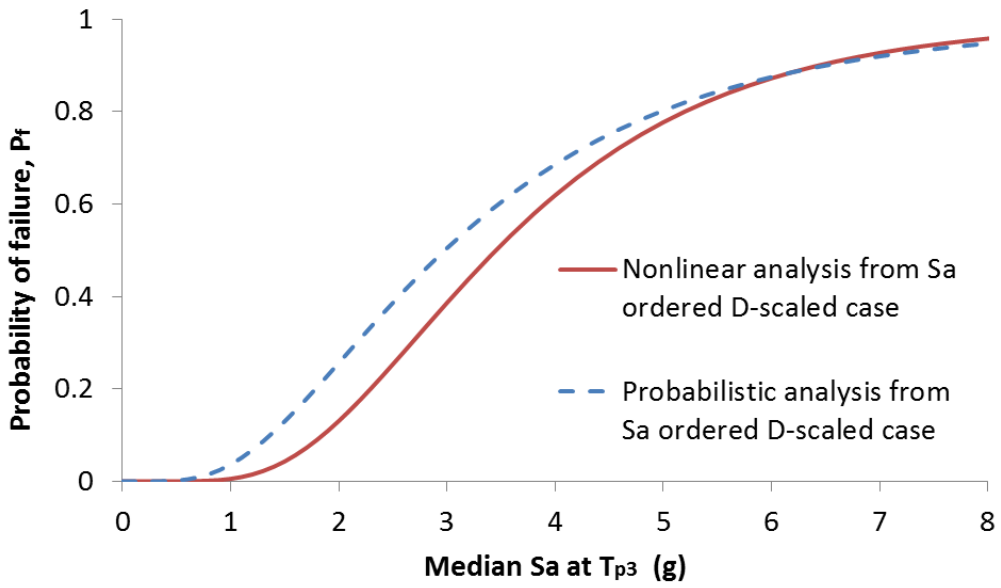

Figure 43: Seismic fragility of piping Tee-joint from SA ordered D-scaled ground motions: nonlinear FE analysis versus probabilistic analysis

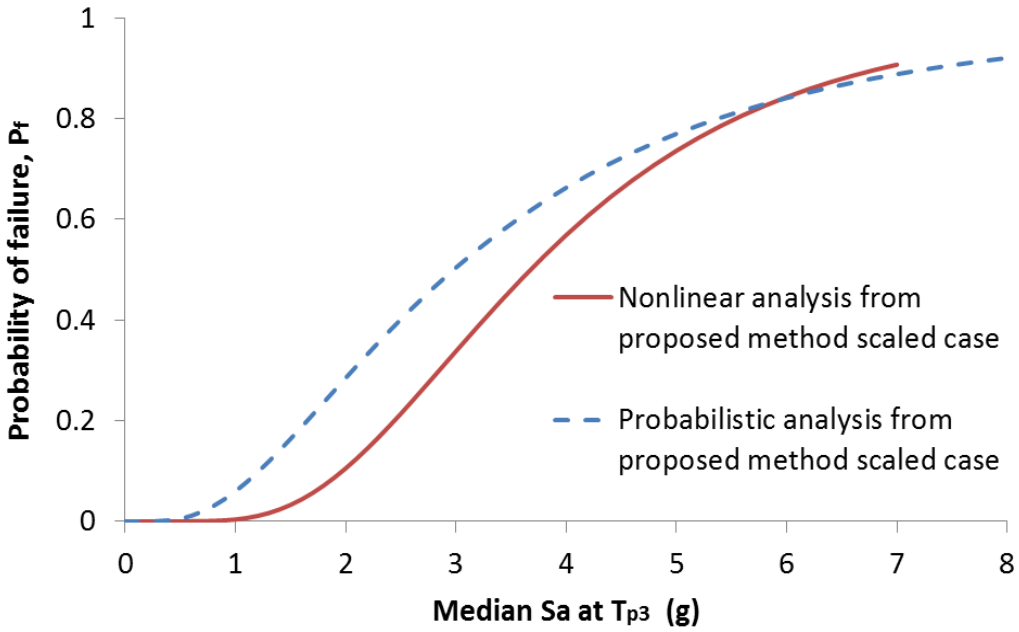

Figure 44: Seismic fragility of piping Tee-joint from proposed-scaled ground motions: nonlinear FE analysis versus probabilistic analysis

PART III: SUMMARY AND CONCLUSIONS

1. Summary and Conclusions

1.1. Summary

Performance based design has been emphasized in ATC-58 and it recommends the use of probabilistic tools and guidelines for seismic risk mitigation. The performance-based seismic design requires the scaling of recorded earthquake ground motions to conduct nonlinear response time history analysis. A key objective of scaling procedure is to preserve the distribution (both the median and the dispersion) in the earthquake shaking for the selected characterization of the hazard to capture behaviors in terms of response for both the structural and the non-structural systems. This paper presents the results from a study that compares and contrasts the characteristics of several frequently used scaling methods as well as a couple of recently proposed methods applying on nonstructural piping systems. A piping model developed from real-life piping system is utilized for finite element analysis in this research, and the failure criterion built from reconciliation of experimental tests and ASME code requirements is considered in the seismic fragility evaluation.

Ground motion scaling is a process of applying a scale factor to each individual record such that its amplitude will be increased or decreased. The main objective of proposing a scale factor is to ensure that the average spectral acceleration of scaled ground motions is not less than the target design response spectrum in the period range of $0.2T_1$ to $1.5T_1$. The design spectrum is increasingly being specified as the Uniform Hazard Spectrum (UHS) in many cases. However, code-based methods are not necessarily suited for performance based design because UHS itself is likely to be excessively conservative for nonlinear time history analysis. It has also been shown that it can under predict the

displacement demand if spectrum compatible artificial records are used in the case of highly nonlinear framing structures. Probabilistic seismic hazard analysis (PSHA) to characterize earthquake hazard is now a widely followed practice, and the selection of a suite of ground motions records is typically based on seismic hazard deaggregation. A key step in the PSHA relates to the characterization of dispersion in seismic shaking by an attenuation relationship which is used to evaluate the median and logarithmic standard deviation of the spectral acceleration at multiple periods.

Nonstructural piping systems display significantly different dynamic features from building structural systems in the sense that fundamental mode (first mode) is not necessarily the significant mode in most cases. Higher order modes which are usually local modes play a significant role in the overall response evaluation. In addition, the behavior of nonstructural systems is highly dependent upon its interaction with the building/structural system that they are attached to.

Four widely used scaling methods are studied in this paper, which are: (i) Single period scaling method, (ii) "Range" based scaling method, (iii) Geometric mean based scaling method, (iv) D-Scaling method. Characteristics of each individual method are analyzed and discussed in this research. A total of 21 ground motions selected using seismic hazard deaggregation are utilized to conduct the nonlinear time-history response analysis. Seismic fragilities of piping system are calculated for each individual scaling method for comparative purposes.

1.2. Conclusions

The main conclusions of this study can be summarized as:

- Single period scaling method is not appropriate in cases where multiple modes of the piping system or piping and building together contribute to the overall performance of the nonstructural systems. Also, application of single period scaling method would be inappropriate fundamental mode of nonstructural system is used for scaling because it is not necessarily the critical mode.
- Single period scaling method would result in a logarithmic standard deviation of zero at scaling period which is intrinsically incorrect in the fragility assessment for any structural and nonstructural piping systems.
- "Range" based scaling method emphasizes scaling ground motions over a broader period range instead of a single period, which gives a relatively better match with the spectral acceleration amplitude as well as the logarithmic standard deviation with target, compared with single period scaling method. However, it underestimates the values of logarithmic standard deviations at low periods which correspond to the higher order piping modes.
- Geometric mean based scaling method preserves the original spectral acceleration shape and original dispersion of unscaled ground motions. However, the logarithmic standard deviation from this method is much larger than that corresponding to the target values and is identical to that conducted from unscaled case.
- D-Scaling method provides a logical and scientific approach that captures not only the median but also the dispersion of spectral acceleration in the selected hazard at a

period of interest. In addition, probabilistic theory is also applied in this method to distribute selected ground motions since median spectral acceleration and logarithmic standard deviation are known. The challenge associated with this method is that the distribution (both the median and logarithmic standard deviation) is preserved merely at single period. Concentrating only on single period makes deficiencies similar to what is given in single period scaling method.

- The D-Scaling method is subjected to non-uniqueness in the sense that the results are highly dependent upon the ordering of ground motions by their magnitudes, PGA values or maximum SA values. Compared with D-Scaling method, the reordering or redistribution of ground motions makes no difference in the shape of scaled spectral accelerations but it would be effective in influencing the shape of scaled logarithmic standard deviation. Magnitude ordered D-Scaling method gives best match with target at the critical mode of the piping system. The deficiency associated with this method is still similar to D-Scaling method, logarithmic standard deviation obtained from PGA ordered D-Scaling as well as SA ordered D-Scaling methods does not match well with the target values in the entire period range of interest.
- Proposed method, known as Geometric Mean based Magnitude ordered D-Scaling Method, gives the most appropriate fragility curve because it allows the best representation of logarithmic standard deviation. This method addressed the problem listed in previous scaling methods and displays a comparably better match with the target of logarithmic standard deviation.

- The piping fragility curves vary significantly based on the scaling method used in nonlinear finite element analyses.
- Most of the scaling methods result in fragility curves that have about the similar median probability of failure but differ significantly in their dispersion. It is evident that the proposed scaling method gives the most appropriate fragility curve because it displays closeness to the target in a broader period range of interest than any other existing scaling methods.

2. Recommendations for Future Research

Based on the experience gained from conducting this study, a few recommendations for future works in this topic are summarized below:

- While the proposed scaling method shows promise for appropriate consideration of logarithmic standard deviation (β), additional work is needed to evaluate its accuracy as well as applicability for many other suites of ground motions.
- It is recommended that the applicability of the proposed method be evaluated for many more types of nonstructural systems particularly the ones with dynamic characteristics that are very different from those of a piping system.
- Ryu (2013) and Tian (2013) show that piping fragility can be significantly influenced by the interaction between the suspended ceiling system and the piping system if the two are connected to each other at sprinkler heads. It is recommended to evaluate the applicability of the proposed method for such a case.

REFERENCES

Ryu, Y. (2013). “Fragility of Piping Systems and Reliability of Piping Components”.

Tian, Y. (2013). “Experimental seismic study of pressurized fire sprinkler piping subsystems”. State University of New York at Buffalo.